



THE UNIVERSITY *of* EDINBURGH

Edinburgh Research Explorer

COMPARISON OF SURFACE AREA AND CORTICAL THICKNESS ASYMMETRY IN THE HUMAN AND CHIMPANZEE BRAIN

Citation for published version:

Li, X, Crow, TJ, Hopkins, WD & Roberts, N 2020, 'COMPARISON OF SURFACE AREA AND CORTICAL THICKNESS ASYMMETRY IN THE HUMAN AND CHIMPANZEE BRAIN', *Cerebral Cortex*.
<https://doi.org/10.1093/cercor/bhaa202>

Digital Object Identifier (DOI):

[10.1093/cercor/bhaa202](https://doi.org/10.1093/cercor/bhaa202)

Link:

[Link to publication record in Edinburgh Research Explorer](#)

Document Version:

Peer reviewed version

Published In:

Cerebral Cortex

General rights

Copyright for the publications made accessible via the Edinburgh Research Explorer is retained by the author(s) and / or other copyright owners and it is a condition of accessing these publications that users recognise and abide by the legal requirements associated with these rights.

Take down policy

The University of Edinburgh has made every reasonable effort to ensure that Edinburgh Research Explorer content complies with UK legislation. If you believe that the public display of this file breaches copyright please contact openaccess@ed.ac.uk providing details, and we will remove access to the work immediately and investigate your claim.



**COMPARISON OF SURFACE AREA AND CORTICAL
THICKNESS ASYMMETRY IN THE HUMAN AND CHIMPANZEE
BRAIN**

Journal:	<i>Cerebral Cortex</i>
Manuscript ID	CerCor-2019-00880.R1
Manuscript Type:	Original Article
Date Submitted by the Author:	01-Jun-2020
Complete List of Authors:	Li, Xiang; University of Edinburgh, Clinical Research Imaging Centre Crow, Tim; SANE POWIC, University Department of Psychiatry Hopkins, William D.; Georgia State University, Neuroscience Institute and Language Research Center Roberts, Neil; University of Edinburgh, Division of Medical and Radiological Sciences
Keywords:	brain asymmetry, chimpanzee, surface area, cortical thickness, species difference

1
2
3
4
5 **COMPARISON OF SURFACE AREA AND CORTICAL THICKNESS ASYMMETRY**
6 **IN THE HUMAN AND CHIMPANZEE BRAIN**
7
8
9

10 Li Xiang^a, Timothy J. Crow^b, William D. Hopkins^c, Neil Roberts^{a*}
11

12
13 ^a School of Clinical Sciences, University of Edinburgh, EH16 4TJ, United Kingdom
14

15 ^b POWIC, University Department of Psychiatry, Warneford Hospital, Oxford, OX3 7JX,
16
17 United Kingdom
18

19 ^c The University of Texas MD Anderson Cancer Centre, Bastrop, Texas 78602, United States
20
21
22
23
24
25
26
27
28

29 Corresponding Author:
30

31 Neil Roberts
32

33 School of Clinical Sciences
34

35 University of Edinburgh
36

37 EH16 4TJ
38

39 United Kingdom
40

41 neil.roberts@ed.ac.uk
42
43
44
45
46
47
48
49
50
51
52
53
54
55
56
57
58
59
60

Abstract

Which structural asymmetries underpin the lateralization of the human brain function can be clarified by comparison with chimpanzees. Here we report the results of vertex-wise and ROI-based analyses that compared surface area (SA) and cortical thickness (CT) asymmetries in 3D MR images obtained for 91 humans and 77 chimpanzees. We find that the human brain has substantially greater asymmetry than the chimpanzee's. Specially, there is (i) larger total SA in the right compared to the left cerebral hemisphere, (ii) a global asymmetry pattern of widespread thicker cortex in the left compared to the right frontal and the right compared to the left temporo-parieto-occipital lobe and (iii) local asymmetries, most notably in the superior temporal sulcus and medial occipital cortex where rightward asymmetry is observed for both SA and CT. There is also (iv) a prominent asymmetry specific to the chimpanzee brain, namely the rightward CT asymmetry in the precentral cortex. These findings provide evidence of there being substantial differences in the asymmetry between the human and chimpanzee brain. The unique asymmetries of the human brain are potential neural substrates for cognitive specializations and the presence of significant asymmetry of precentral gyrus in the chimpanzee brain should be further investigated.

Key words: brain asymmetry, chimpanzee, cortical thickness, surface area.

1. Introduction

A key feature of the human brain is the population-level functional and structural asymmetry. Clinical and experimental data obtained using a variety of methods have documented the left hemispheric specializations for linguistic and praxis functions (Knecht et al., 2000; Ocklenburg & Gunturkun, 2018). Several structural asymmetries have been identified in the human brain and are potential neural substrates for the functional lateralization (e.g., Barrick, Lawes, Mackay, & Clark, 2007; Josse, Kherif, Flandin, Seghier, & Price, 2009). For example, the Sylvian fissure typically rises more steeply in the right cerebral hemisphere and extends further posteriorly in the left cerebral hemisphere (Cunningham, 1892; Eberstaller, 1884, 1890; Ide, Rodriguez, Zaidel, & Aboitiz, 1996; Rubens, Mahowald, & Hutton, 1976; Yeni-Komshian & Benson, 1976), and the planum temporale (PT), which is the flat surface of the posterior superior temporal gyrus posterior to Heschl's gyrus, is larger on the left compared to the right in a statistical majority of humans (Geschwind & Levitsky, 1968; Shapleske, Rossell, Woodruff, & David, 1999; Vadlamudi et al., 2006; Witelson & Kigar, 1988). Also notable in the human brain is the so-called torque whereby there is a global anti-clockwise twist in the transverse plane. Its exaggerated posterior component in terms of the protrusion and rightward bending of the left occipital lobe (LeMay, 1982; Witelson and Kigar, 1988; Xiang et al., 2018) is potentially related to the greater posterior extension of the lateral ventricle in the left compared to the right cerebral hemisphere (Narr et al., 2001). A list of brain structural asymmetry studies is provided in Table 1, however, in no means to be comprehensive. Historically, asymmetries in brain structure, cognitive and motor functions have been considered uniquely human and presumed to be evolved after the split from the common ancestor of humans and great apes (Bradshaw & Rogers, 1993; Corballis, 1992; Corballis, 2002; Crow, 2009). However, research over the past 20 to 25 years has challenged this long held view with a growing body of evidence demonstrating asymmetries in non-human animals (Corballis, 2009; Ocklenburg & Gunturkun, 2018; Rogers, Vallortigara, & Andrew, 2013). Nevertheless, fundamental questions that persist are whether there are some asymmetries of the human brain evolved after the separation from the common ancestor with primates and underpinning the human specific adaptation and cognitive ability? The search of such human-specific features is best determined through comparative study with our closest living relative - the chimpanzee (Rilling et al., 2011).

1
2
3
4
5
6
7
8
9
10
11
12
13
14
15
16
17
18
19
20
21
22
23
24
25
26
27
28
29
30
31
32
33
34
35
36
37
38
39
40
41
42
43
44
45
46
47
48
49
50
51
52
53
54
55
56
57
58
59
60

As with many comparative brain studies, identifying species-specific features of lateralization is challenging given the substantial variation in the overall size of the brain and the definition of anatomical regions of interest (ROI) in different species (Keller, Deppe, Herbin, & Gilissen, 2012; Keller et al., 2007). In addition, different computational methods may be adopted for the quantification of brain measures for difference species, which makes the comparison difficult. Based on brain mapping techniques, surface-based morphometry (SBM) analysis enables the projection of brains of difference size to a common standard so that the established inter-subject correspondence allows direct comparison between subjects across the whole cortical surface on a vertex-by-vertex basis. For the examination of inter-hemispheric brain asymmetry, Greve et al. (2013) further proposed an approach to establish the inter-hemispheric correspondence by projecting both cerebral hemispheres to a left-right symmetric registration atlas. The pipeline has been integrated in the FreeSurfer suite and gained popularity in the study of human brain asymmetry. However, relevant application on the chimpanzee brain is very few in the literature. In our previous brain morphology study (Xiang, Crow, & Roberts, 2019a, 2019b; 2018), we adopted Greve's approach to compare the inter-hemispheric positional brain asymmetry between humans and chimpanzees under the same framework. The findings suggested absence of cerebral torque in the chimpanzee brain, contradict to the previous literature (Balzeau & Gilissen, 2010; Hopkins & Marino, 2000; LeMay, 1982). In the present study, we have extended our research and examined the asymmetry of two fundamental measurements which characterize the cerebral cortex, namely surface area (SA) and cortical thickness (CT).

Based on pre-labelled atlases, such as the Desikan-Killiany atlas (Desikan et al., 2006) in the FreeSurfer Image Analysis Suite (<http://surfer.nmr.mgh.harvard.edu>), brain measures can be summarized in particular ROIs. Specially, there are two parcellation atlases independently constructed for the left and right cerebral hemispheres based on the corresponding manual labelling of a series of brain images. In many studies, these two atlases were employed to separately compute regional value for each cerebral hemisphere and the asymmetry was the difference between values of hemispheres. Given the regional computation procedure relies on two standards, i.e. one atlas for each cerebral hemisphere, we refer this conventional approach as a two-atlas parcellation scheme (TAPS). However, as shown in Figure S1 (a) of the Supplementary Materials, there is significant areal difference between the left and right side of the Desikan-Killiany atlas that reflects the inherent asymmetry of the human brain and as demonstrated in Figure S1 (b) in the Supplementary Materials, different

1
2
3 numbers of vertices are thereby assigned to corresponding ROIs in the left and right cerebral
4 hemispheres of the atlas. More vertices are allocated to the ROI of larger area than to the
5 smaller area. For example, there are 1454 vertices in the larger left PT in comparison to 1022
6 vertices in the smaller right PT according to Destrieux atlas (Destrieux, Fischl, Dale, & Halgren,
7 2010). We are concerned that the areal asymmetry in the atlas may be propagated to the
8 regional parcellation for individual subjects and systematically affect the result of brain
9 regional measures through differentially distributed vertices. Indeed, in a TAPS-based meta-
10 analysis based on a “largest ever” population of healthy human subjects, Kong et al. (2018)
11 reported much lower variability of SA asymmetry in comparison to that of CT across many
12 databases. Whilst the authors associated the observation with the computation scheme (i.e.
13 TAPS), we agree and specify that the high consistency of SA measures implies strong influence
14 of bias in the parcellation atlas to brain regional analysis. At the stage, this atlas-bias has not
15 yet been evaluated. A new approach for the ROI-based asymmetry analysis is necessary if ROI
16 analyses are to be considered robust.
17
18
19
20
21
22
23
24
25
26
27
28
29

30 **Insert Table 1 here**
31
32
33
34
35

36 The main objective of the present study is to perform a comparative analysis of SA and
37 CT asymmetry between the human and chimpanzee brain. Firstly, the global inter-hemispheric
38 SA and CT asymmetries were examined and compared between species. Secondly, SA and CT
39 asymmetries were accessed on a vertex-by-vertex basis. Thirdly, a novel approach was
40 developed for the ROI-based asymmetry analysis which we have named single-atlas
41 parcellation scheme (SAPS). Compared to TAPS, SAPS additionally employs the established
42 vertex-wise correspondence between the left and right cerebral hemispheres and therefore is
43 able to project the anatomical convention from a single parcellation atlas (e.g. left or right side
44 of the parcellation atlas) to both the corresponding and the contralateral cerebral hemispheres
45 of individual subjects.
46
47
48
49
50
51
52
53
54
55
56
57
58
59
60

2. Methods

2.1 Subjects and MRI Data Acquisition

MR imaging of humans was conducted at the Queen's Medical Research Institute (QMRI), University of Edinburgh, UK and the Oxford Centre for Magnetic Resonance (OCMR), University of Oxford, UK. Altogether, there are 91 healthy subjects (39 females and 52 males, average age 33.5 ± 12.0 years) in the study, 42 recruited in Edinburgh and 49 recruited in Oxford. Handedness information was recorded for 31 subjects in the Edinburgh group, in which four are left-handed, two have ambiguous handedness and the rest are right-handed, and for 47 subjects in the Oxford group, in which two are left-handed and the rest are right-handed. MR imaging of chimpanzees was conducted at Yerkes National Primate Research Centre (YNPRC) in Atlanta, Georgia, US. There are 77 chimpanzees (50 females and 27 males, average age 26.2 ± 14.0 years). Approval for this study was obtained separately at each site from the local Research Ethics Committee and human subjects provided fully informed written consent prior to taking part.

In Edinburgh the MR images of human subjects were acquired using a 3 T Verio MRI system (Siemens Medical Systems, Erlangen, Germany) and acquisition parameters for the 3D T1-weighted Magnetization-Prepared Rapid-Acquisition Gradient Echo (MPRAGE) sequence are TR = 2300 ms, TE = 2.98 ms, TI = 900 ms, Flip angle = 9° , FOV = 256 mm x 256 mm and the images have isotropic voxel resolution of 1 mm. In Oxford the MR images of human subjects were acquired using a 1.5 T Sonata MRI system (Siemens Healthineers, Erlangen, Germany) and the acquisition parameters for the 3D T1-weighted fast low-angle shot (FLASH) sequence are TR = 5400 ms, TE = 76 ms, Flip angle = 90° , FOV = 256 mm x 160 mm and the images have isotropic voxel resolution of 1mm. In Atlanta the MR images for the chimpanzees were acquired using a Siemens 3 T Trio MRI system (Siemens Healthineers, Erlangen, Germany) and acquisition parameters for the 3D T1-weighted MPRAGE sequence are TR = 2300 ms, TE = 4.4ms, TI = 1100ms, flip angle = 8° , FOV = 200 mm x 200 mm, data matrix size of 320 x 320 and the images have isotropic voxel resolution of 0.6 mm. The chimpanzees were immobilized by ketamine injection (10 mg/kg) and subsequently anesthetized with propofol (40–60 mg/kg/hr) before transportation to the MRI facility where they were scanned supine with a human head-coil and remained anesthetized (total time ~2 hours) for the MR imaging before returning to the home compound.

2.2 Image Analysis

All MR images were pre-processed in FSL (version 5.0.9, <http://fsl.fmrib.ox.ac.uk/fsl/fslwiki/>) including skull strip, bias field correction and brain normalization using a 7 degrees of freedom (DoF) transformation including 3 translations, 3 rotations and 1 uniform scaling. Specially, the normalization step registered all brain volume images, particularly the chimpanzee brains, to the standard human MNI152 template while preserving the morphology of the brain. Thereby these pre-processed brains were able to be subsequently put through the standard FreeSurfer pipeline (version 6.0, <https://surfer.nmr.mgh.harvard.edu/>). In FreeSurfer, a volumetric analysis was firstly performed to label the white matter of the brain and split the brain into two cerebral hemispheres. Secondly, a triangular mesh was generated and deformed to tightly cover the white matter component for each cerebral hemisphere with respect to the intensity gradients between the white matter and grey matter and this mesh is the so-called white matter surface. Thirdly, the white matter surface continued to expand along the direction of the intensity gradients between the gray matter and CSF until it coincided with gray matter surface and this surface is also referred to as the so-called pial surface (Dale 1999). For quality control, we visually inspected the reconstructed brain surface for all subjects.

2.3 Vertex-wise Analysis of Brain Asymmetry

For vertex-wise analysis, as described in (Greve et al., 2013; see also Figure 1 (a)), the inter-hemispheric and between-subject correspondences were established through a non-linear registration that adjusts the vertex coordinates of both the left and right cerebral hemispheres of individual subjects to match the folding pattern (i.e. curvature) of a pre-trained left-right symmetric registration atlas (e.g. lh.fsaverage_sym in FreeSurfer which refers to a symmetric atlas constructed based on an initial left hemispheric atlas) in spherical space. In the case of the human brain, the symmetric registration atlas was already available in FreeSurfer (e.g. lh.fsaverage_sym). Whereas the atlas of the chimpanzee brain was specifically constructed for this study based on the procedure described in (Greve et al., 2013). In brief, for 30 brains selected at random from the chimpanzees cohort: (i) both cerebral hemispheres of each subject were co-registered to an initial left-right symmetric atlas (i.e. lh.fsaverage_sym); (ii) a new atlas was generated by averaging the aligned folding patterns of the left and right hemispheres

1
2
3 for all the subjects in the training pool and (iii) the process was iterated three times to produce
4 the final left-right symmetric registration atlas for the chimpanzee brain. Based on the
5 established correspondences, surface-based measures, i.e. SA and CT, that were resampled to
6 the reference atlas space were compared between hemispheres and across subjects. In particular,
7 surface-based spatial smoothing was performed to increase the signal-to-noise ratio. As shown
8 in Figure S4 of the Supplementary Materials, the asymmetry pattern remains the same under
9 different filter sizes and specially, a Gaussian filter with full-width half-maximum (FWHM) of
10 15 mm was chosen as it corresponds well with the size of brain petalia and gyri which are the
11 features that are the focus of interest in the study.
12
13
14
15
16
17
18
19
20
21

22 **Insert Figure 1 here**
23
24
25

26 ***2.4 ROI-based Analysis of Brain Asymmetry*** 27

28 Firstly, the influence of the atlas-bias in the traditional TAPS-based analysis was
29 investigated. We performed an experiment in which the Desikan-Killiany atlas was applied to
30 measure brain asymmetry in a subset of 14 individuals randomly selected from the human
31 cohort. In particular, the TAPS analysis pipeline was applied to the original 3D MR images of
32 the brain and also to the left-right flipped version of the 3D MR images. As demonstrated in
33 Figure S2 (b) of the Supplementary Materials, 23 of 34 (67.7%) ROIs remain to be in the same
34 asymmetry direction even after the image being flipped and these ROIs overlap with the
35 regions showing the largest atlas bias (see Figure S1 (b) of the Supplementary Materials),
36 suggesting that the atlas-bias significantly influences the result of brain asymmetry when TAPS
37 is used. In addition, positive rather than negative correlation was found between the regional
38 SA asymmetries computed for the original scans and their flipped versions [$r=0.79$, $p<0.001$],
39 and both of which are highly positively correlated to the corresponding asymmetry of the
40 Desikan-Killiany atlas (i.e. asymmetry of number of vertices distributed in corresponding ROIs
41 in the left and right cerebral hemisphere [$r>0.70$, $p<0.001$]), which may explain the high
42 consistency of SA asymmetry across databases observed by Kong et al. (2018). We believe
43 that the CT asymmetry is comparatively less severely affected because that the atlas-bias is
44 inherently an areal difference between hemispheres and also, whilst the SA measures are
45 computed as a sum of values at individual vertices within each ROI the CT measures are
46 computed by means of averaging in which the effect bias is eliminated.
47
48
49
50
51
52
53
54
55
56
57
58
59
60

1
2
3
4
5
6
7
8
9
10
11
12
13
14
15
16
17
18
19
20
21
22
23
24
25
26
27
28
29
30
31
32
33
34
35
36
37
38
39
40
41
42
43
44
45
46
47
48
49
50
51
52
53
54
55
56
57
58
59
60

In order to address the above atlas-bias in TAPS-based analysis, we developed a new single-atlas parcellation scheme (SAPS), in which only one parcellation standard is employed at one time to subdivide both cerebral hemispheres of individual subjects. As demonstrated in Figure 1 (c), the regional labels of the left side of the Desikan-Killiany atlas were assigned to both the ipsilateral and contralateral cerebral hemispheres of individual subjects based on their inter-hemispheric correspondence as described in Section 2.3. This approach inherently sets a constraint whereby an identical number of vertices is assigned to the corresponding ROI in each cerebral hemisphere. Whilst in TAPS, as shown in Figure 1 (b), the parcellation convention of each cerebral hemisphere in the Desikan-Killiany atlas can only be projected to the corresponding hemisphere of individual subjects based on the between-subject correspondence (see Figure 1 (d)) but no connection between cerebral hemispheres was built. Although vertex-wise analysis has been shown to be less prone to choice of left or right side of the registration atlas (i.e. lh.fsaverage_sym or rh.fsaverage_sym, Greve et al. 2013), there is still concern on the projection of regional parcellation to contralateral cerebral hemisphere. Therefore, the same analysis pipeline was repeated but now using the right side of the Desikan-Killiany atlas for brain parcellation and the right side of the FreeSurfer atlas (i.e. rh.fsaverage_sym which refers to a symmetric atlas constructed based on an initial right hemisphere atlas) for the inter-hemispheric co-registration in the vertex-wise analysis. The ROI-based values of SA and CT were thereby an average of the values respectively computed based on the left and right atlases. We visually inspected the surface parcellation results for all the human and chimpanzee subjects. Examples for 10 randomly selected chimpanzee subjects are shown in Figure S3 of Supplementary Materials, which demonstrates that the Desikan-Killiany atlas provides reasonable parcellation results for the chimpanzee brain.

Insert Figure 2 here

2.5 Statistical Analysis

In all of the analyses (i.e. global, vertex-wise and ROI), the asymmetry index (AI) was defined as the normalized difference between the left and right cerebral hemisphere according to the formula of $AI = 2*(L-R)/(L+R)$. For the global and ROI-based analyses, two-tailed one sample *t*-tests and multivariate analysis of variance (MANOVA) were respectively performed to test the significance of inter-hemispheric asymmetry of SA and CT for each species and

1
2
3 examine the sex effect on asymmetries using SPSS Statistics for Mac, Version 22.0 (IBM Corp.,
4 Armonk, N.Y., USA). For the vertex-wise analysis, GLM in FreeSurfer was performed at each
5 cortical location on the cerebral surface to identify the clusters of significant SA and CT
6 asymmetries respectively for the human and chimpanzee brains and the regions showing
7 significant between-species difference, followed by a cluster-wise multiple comparison with
8 both the cluster forming and cluster-wise significant levels being set to 0.01. In addition, the
9 Spearman's correlation analysis was performed to explore the consistency of directional
10 asymmetry between the human and chimpanzee brain based on the ranked order of the
11 asymmetry indices across 34 ROIs of the Desikan-Killiany atlas.
12
13
14
15
16
17
18
19
20
21
22
23
24
25
26
27
28
29
30
31
32
33
34
35
36
37
38
39
40
41
42
43
44
45
46
47
48
49
50
51
52
53
54
55
56
57
58
59
60

For Peer Review

3. Results

3.1 Global SA and CT asymmetry

The mean values of SA and CT in the left and right cerebral hemispheres are presented in Table 2 for the human and chimpanzee brain. For the human brain, total SA is significantly larger in the right compared to the left cerebral hemisphere [$t(90) = -4.10$, $p < 0.001$] but there is no significant population-level asymmetry for CT. For the chimpanzee brain, no significant population-level asymmetry was found for either SA or CT. MANOVA showed no main effect of sex on SA or CT asymmetry in either the human [$F(2,88) = 1.23$, $p = 0.30$] or chimpanzee [$F(2,74) = 0.67$, $p = 0.52$] brain.

3.2 Vertex-wise and ROI-based SA Asymmetry

According to Figure 2 (a), the vertex-wise analysis for the human brain revealed significant rightward SA asymmetry in the (i) STS extending to posterior insula, (ii) inferior parietal and (iii) medial frontal and (iv) medial occipital cortex. In contrast, significant leftward asymmetry was found in the (v) supra-marginal gyrus extending to PT and (vi) anterior insula extending to Broca's area and anterior and inferior temporal lobe. In comparison, the vertex-wise analysis for the chimpanzee brain showed significant leftward asymmetry in the (i) Sylvian fissure extending from anterior superior temporal to supra-marginal gyrus and (ii) inferior parietal cortex and cuneus, but there are no significant population-level rightward asymmetries. The comparative analysis further revealed significant species difference in the (i) STS, (ii) posterior insula, (iii) inferior parietal, (iv) inferior temporal, (v) medial frontal and (vi) medial occipital and (vii) supra-marginal gyrus. According to the average SA asymmetry map computed for individual species in Figure 4 (a), only the species difference in the supra-marginal gyrus is due to a magnitude difference while in the remaining regions, SA asymmetries are in opposite directions between the human and chimpanzee brain.

The result of the ROI-based analysis of SA asymmetry is depicted in Figure 3 (a). There are a greater number of ROIs showing significant asymmetry in the human brain (i.e. in 10 of 34 ROIs) compared to the chimpanzee brain (i.e. in 2 of 34 ROIs). The statistics of regional SA asymmetries are summarized in Table 3 and the measurements of SA for the 34 ROIs per cerebral hemisphere of the Desikan-Killiany atlas are provided in Table S1 of the Supplementary Materials respectively for the human and chimpanzee brain.

MANOVA revealed no significant main effect of sex on the overall SA asymmetry in either the human [$F(34,56) = 1.51$, $p = 0.08$] or chimpanzee [$F(34,42) = 0.92$, $p = 0.60$] brain. Although, subsequent univariate ANOVA showed significant effect of sex on SA asymmetry

1
2
3 in the superior temporal lobe [$F(1,89) = 9.56, p = 0.003$], cuneus [$F(1,89) = 5.61, p = 0.02$],
4 pars opercularis [$F(1,89) = 4.75, p = 0.03$] and pars triangularis [$F(1,89) = 8.19, p = 0.01$] for
5 the human brain and in bankssts [$F(1,75) = 5.39, p = 0.02$] and inferior parietal [$F(1,75) = 4.11,$
6 $p = 0.05$] for the chimpanzee brain, however, none survived Bonferroni correction for multiple
7 comparisons.
8
9
10
11
12

13 **3.3 Vertex-wise and ROI-based CT Asymmetry**

14
15 According to Figure 2 (b), the vertex-wise analysis of CT asymmetry for the human
16 brain revealed significant rightward asymmetry in the (i) temporal and (ii) occipital lobes and
17 significant leftward asymmetry in the (iii) superior and middle frontal gyrus. In comparison,
18 the vertex-wise analysis for the chimpanzee brain revealed significant rightward asymmetry in
19 the (i) pre-central gyrus, (ii) paracentral gyrus and significant leftward asymmetry in the (iii)
20 dorsal anterior cingulate. The comparative analysis further revealed significant species
21 differences in the (i) STS, (ii) medial occipital and (iii) pre-central cortex. According to the
22 average asymmetry map computed for individual species shown in Figure 4 (b), in all these
23 areas exhibiting significant species difference, CT asymmetries are in opposite directions
24 between the human and chimpanzee brain.
25
26
27
28
29
30
31
32

33 The results of the ROI-based analysis of CT asymmetry is depicted in Figure 3 (b).
34 There are 9 out of 34 ROIs showing significant population-level asymmetry in the human brain
35 compared to 7 out of 34 ROIs in the chimpanzee brain. The statistics of regional CT asymmetry
36 are shown in Table 4 and the measurements of CT for the 34 ROIs per cerebral hemisphere of
37 the Desikan-Killiany atlas are summarized in Table S2 of the Supplementary Materials for the
38 human and chimpanzee brain. Most notably, both the vertex-wise and ROI-based analysis
39 showed that the frontal lobe is thicker in the left compared to the right cerebral hemisphere and
40 the temporo-parieto-occipital lobe is thicker in the right compared to the left cerebral
41 hemisphere in the human brain, a pattern that is not present in the chimpanzee brain.
42
43
44
45
46
47

48 MANOVA revealed no significant main effect of sex on CT asymmetry in either the
49 human [$F(34,56) = 0.79, p=0.76$] or chimpanzee [$F(34,42) = 0.54, p = 0.97$] brain, neither did
50 subsequent ANOVA in any ROIs.
51
52
53
54

55 **Insert Figure 2 here**

56 **Insert Figure 3 here**

57 **Insert Figure 4 here**
58
59
60

3.4 Relationship between Asymmetries in the Human and Chimpanzee Brain

We are also interested in whether variation in the direction and magnitude of asymmetries in SA and CT are similar or different between the human and chimpanzee brain. The correlation analysis revealed that for CT, but not SA, there is modest and marginally significant consistency in the strength and direction of asymmetries across 34 ROIs between humans and chimpanzees [CT: $r = 0.34$, $p = 0.05$; SA: $r = 0.15$, $p = 0.40$]. Whereas the correlation analysis between SA and CT asymmetry showed that on average there is no significant relationship between SA and CT asymmetry in either the human [$r = 0.08$, $p = 0.64$] or the chimpanzee [$r = 0.31$, $p = 0.08$] brain.

For Peer Review

4. Discussion

We performed a comparative study of SA and CT asymmetries in the human and chimpanzee brain. Overall, the results revealed that asymmetries are more extensive in the former than the latter given that globally, there is significantly greater SA in the right compared to the left cerebral hemisphere in and only in the human brain, and locally, population-level SA asymmetry was observed in 10 of 34 (29.4%) ROIs and CT asymmetry in 9 of 34 (26.5%) ROIs for the human brain, compared with respective values of 2 of 34 (5.9%), and 7 of 34 (20.6%) ROIs for the chimpanzee brain. In addition, there is significant difference between the human and chimpanzee brain and it largely arises from the difference in the pattern of asymmetry rather than the difference in the magnitude of asymmetry between species. In particular, human-specific population-level SA asymmetries were found in the STS, insula, supra-marginal gyrus, inferior parietal, medial occipital, medial orbital frontal and anterior cingulate and CT asymmetries in the middle temporal and medial occipital gyrus, whereas chimpanzee-specific population-level asymmetry was observed only in the pre-central gyrus for CT.

In the present study we addressed the atlas-bias in the conventional ROI-based analysis. Specially, a novel parcellation scheme called SAPS was developed for the regional analysis. The development of the SAPS approach as compared to the TAPS approach is broadly equivalent to the use of a symmetric compared to a standard atlas in Voxel Based Morphometry (VBM) studies. In particular, when an atlas is developed by using the image registration technique to combine the images of individuals in a cohort, if there is an average asymmetry in the population this will appear in the atlas (see Figure S1 of the Supplementary Materials). If the atlas is then used in a new study this asymmetry can potentially add asymmetry to a population of individuals in which no asymmetry is present. Since our previous studies have shown that the chimpanzee brain is more symmetrical than the human brain (e.g. Xiang et al., 2018) we had concerns that by using TAPS the inherent asymmetry of the human Desikan-Killiany atlas could be propagated to the chimpanzee brain. In SAPS, because an equivalent number of vertices is assigned to refer to each ROI in the left cerebral hemisphere and the corresponding ROI in the right cerebral hemisphere, it limits the propagation of asymmetry that may arise from there being different numbers of vertices associated with the corresponding ROI's in the left or right cerebral hemisphere (see Figure S1 (b) of the Supplementary Materials). In addition, the averaging which occurs as the last step in the SAPS analysis resembles the construction of a symmetric atlas in the VBM approach (i.e. an averaging between the standard atlas and its mirror reflection). For each ROI, measurements derived from

1
2
3 the left and right sides of the parcellation atlas are averaged to avoid the possibility of bias if
4 only one side had been used. Demonstration that SAPS provides a less biased approach for the
5 ROI-based analysis of cerebral asymmetry is provided in Figure S2 of the Supplementary
6 Materials. In brief, the analysis pipeline of SAPS was applied to the original 3D MR images of
7 14 brains and also to left-right flipped versions of the same images. In Figure S2 it can be
8 clearly seen that the results are almost completely reversed in the case when SAPS is used but
9 not when TAPS is used. This observation is supported quantitatively in that the SA asymmetry
10 measurements remained in the same direction in 23 of 34 ROIs (i.e. 67.7%) when TAPS was
11 used but only in 4 of 34 ROIs (11.8%) when SAPS was applied. In addition, whilst the regional
12 SA asymmetries computed using TAPS are highly determined by the asymmetry in the
13 Desikan-Killiany atlas ($r > 0.7$, $p < 0.005$), i.e., asymmetry of number of vertices distributed in
14 corresponding ROIs in the left and right cerebral hemisphere, this is not the case when using
15 SAPS, which further demonstrates that the latter is less prone to the atlas-bias.

16
17
18
19
20
21
22
23
24
25
26 Regarding the SA asymmetry in the human brain, in agreement with the meta-analysis
27 performed by Kong et al. (2018), we found that the total brain SA is significantly larger on the
28 right cerebral hemisphere compared to the left, and there is leftward asymmetry in the
29 transverse temporal gyrus, superior temporal, inferior temporal, supra-marginal gyrus and
30 rightward asymmetry in the middle temporal cortex, inferior parietal, cuneus and peri-calcarine.
31 However, we failed to reproduce the rightward asymmetry in the anterior and leftward
32 asymmetry in the posterior Broca's area, where show the largest atlas-bias (see Figure S1 of
33 the Supplementary Materials). In addition, the finding of significant leftward asymmetry of a
34 region in the anterior Broca's area extending to the lateral orbital frontal and anterior temporal
35 cortex is consistent with the observation in another vertex-wise analysis by Lyttelton et al.
36 (2009), and significant leftward asymmetry of the parahippocampal gyrus and significant
37 rightward asymmetry of the medial orbital frontal are consistent with the findings by Van Essen
38 et al. (2012). In the case of CT asymmetry, a marked pattern was found in the human brain,
39 corresponding to the relatively thicker gray matter cortex in the left compared to the right
40 frontal lobe and the right compared to the left temporo-parieto-occipital lobe which forms the
41 pattern of torque. This finding is consistent with the observations by Plessen et al. (2014),
42 Luders et al. (2006) and Le Guen et al. (2018b), however, opposite to the findings of Zhou et
43 al. (2013) and Maingault et al. (2016). Lateralization has also been reported for the white matter
44 underlying the gray matter. For example, the white matter (i.e. arcuate fasciculus) which links
45 lateral temporal cortex and frontal lobe has been reported to be both structurally and
46 functionally asymmetric (Takaya et al., 2015; Trivedi et al., 2009). Furthermore, Rilling et al.
47
48
49
50
51
52
53
54
55
56
57
58
59
60

1
2
3 (2011) reported that there has been a remarkable augmentation of this dorsal language pathway
4 in human evolution, and which is more pronounced in the left hemisphere and is suggested to
5 be related to the development of language. The potential relationship between the asymmetry
6 of the gray matter and white matter is an important topic for further investigation.
7
8
9

10 Two brain areas were found to be asymmetric in both the SA and CT analyses in the
11 human brain. They are the medial occipital lobe and STS. Both showed reduction of SA and
12 CT on the left compared to the right. In the case of the medial occipital lobe, the observation
13 is compatible with the greater posterior extension and rightward bending that were previously
14 reported in the occipital lobe (Xiang et al., 2018) and rightward gyrification asymmetry in the
15 associated region was also reported by Chiarello et al. (2016). In the case of STS, the finding
16 supports the superior temporal asymmetrical pit (STAP) asymmetry identified by Leroy et al.
17 (2015) as the “new human specific landmark”, which has been later found to be genetically
18 constrained (Le Guen et al., 2018a; Le Guen et al., 2018b), advocating its potential role for the
19 language specification developed during very recent evolution. Of further interest with respect
20 of the human brain is the finding of opposite directions of SA asymmetry in the anterior (i.e.
21 leftward) and posterior insula (i.e. rightward). This finding may help to resolve the discrepancy
22 between asymmetries previously reported for this brain region. In particular, Watkins et al.
23 (2001) performed a VBM-based asymmetry study in 142 healthy subjects and reported
24 significant rightward asymmetry whereas Keller et al. (2011) performed a stereological
25 analysis to measure insula volume in 25 subjects with confirmed hemisphere language
26 dominance (HLD) and reported leftward insula asymmetry to be associated with left HLD. The
27 respective blue and red coloured regions overlying the anterior and posterior insula in the
28 second panel of the top row of Figure 2 and which are compatible with the respective findings
29 of Watkins et al. (2001) and Keller et al. (2011), respectively, and not present in the results of
30 the ROI-based analysis of the first panel of the same row, indicate that the averaging inherent
31 in the use of predefined ROI's may obscure findings of interest.
32
33
34
35
36
37
38
39
40
41
42
43
44
45
46
47

48 The chimpanzee brain shows less areas of significant population-level SA and CT
49 asymmetry than the human brain and no significant population-level asymmetry in the global
50 SA and CT. In contrast to previous post-mortem studies by Hopkins and Avants (2013), and
51 Cantalupo and Hopkins (2001), we did not find extensive CT asymmetry in frontal, parietal
52 and temporal lobes, except for the rightward asymmetry in the pre-central gyrus, and
53 significant leftward SA asymmetry of the Broca area, respectively. The observation of
54 significant rightward CT asymmetry in the pre-central gyrus specific to the chimpanzee brain
55 is a new finding. Larger proportionally compared to Old World monkeys, the primary motor
56
57
58
59
60

1
2
3 region of the chimpanzee brain has the thinnest cortex across the whole cerebral surface
4 (Hopkins & Avants, 2013; Hopkins et al., 2016). After taking account of brain size, it is also
5 disproportionately thinner than in humans (Hopkins et al., 2016). At the cellular level, a post-
6 mortem study of 18 chimpanzees revealed that the density asymmetry of parvalbumin-
7 immunoreactive interneurons in layers II and III of primary motor cortex to be significantly
8 related to hand preference (Sherwood, Wahl, Erwin, Hof, & Hopkins, 2007). These evidences
9 suggest that structural asymmetry of primary motor cortex may be related to the evolution of
10 handedness (Hopkins & Cantalupo, 2004). Nevertheless, cautions still need be taken in
11 interpreting the functional significance of this asymmetric feature. Because on the one hand
12 the present study showed humans who have more definite handedness preference do not
13 present any asymmetry in this region. On the other hand, large sample size studies of humans
14 have also failed to find significant association between asymmetry of primary motor cortex
15 and handedness (Good et al., 2001; Kong et al., 2018; Wiberg et al., 2019), nor any cortical
16 structural correlates of handedness (Guadalupe et al., 2014).

17
18
19
20
21
22
23
24
25
26
27
28
29
30
31
32
33
34
35
36
37
38
39
40
41
42
43
44
45
46
47
48
49
50
51
52
53
54
55
56
57
58
59
60
The present study provides substantial evidence on that humans and chimpanzees show
different patterns of asymmetry. Specially, the direction of asymmetry in the region showing
significant species difference is on average opposite between the human and chimpanzee brain
(see Figure 4). In addition, the species difference in most cases arises from distinctive
asymmetry in the human brain which is absent in the chimpanzee brain on a population-level,
with one exception in the pre-central cortex. In this context, the divergence of asymmetry found
here challenges the view of gradual process of evolution in which chimpanzees are considered
to share the same pattern of asymmetry as humans but only differ in a matter of magnitude
(Gomez-Robles, Hopkins, & Sherwood, 2013). The presence of asymmetries in the
chimpanzee brain, though few in number, also provides further confirmation that population-
level asymmetry is not unique to *Homo sapiens*. Population-level behavioural, functional and
anatomical asymmetries have been previously reported in a wide range of primates (Corballis,
2009; Holloway & De La Costelareymondie, 1982; Hopkins, Misiura, Pope, & Latash, 2015).
Holloway and De La Coste-Lareymondie (1982) were the first to study brain asymmetry in
pongids (i.e. great apes) and hominids (i.e. humans and their fossil ancestors). They reported
that while all taxa of hominoids (i.e. both groups) show asymmetries to various degrees, the
patterns or combination of petalial asymmetries are very different. Only modern *Homo* and
hominids (*Australopithecus*, *Homo erectus*, Neandertals) show a distinct left-occipital, right-
frontal petalial asymmetry pattern. Of the pongids, gorilla shows leftward asymmetry of the
occipital petalias. Subsequently, in a study of formalin fixed brain specimens of 5 Old and New

1
2
3 World Monkey species, Heilbroner and Holloway (1988) reported significantly greater Sylvian
4 fissure length in the left compared to the right cerebral hemisphere, as is typical in humans
5 (Hou et al., 2019), in four of the species. Corresponding population-level leftward asymmetries
6 of PT have also been reported for chimpanzees (Gannon, Holloway, Broadfield, & Braun, 1998;
7 Hopkins & Nir, 2010; Zilles et al., 1996) and baboons (Marie et al., 2017) but not in macaque
8 monkeys (Gannon, Kheck, & Hof, 2008; Lyn et al., 2011). Hopkins et al., (2015) have
9 investigated whether hemispheric specialization evolved as a by-product of increasing brain
10 size relative to the surface area of the corpus callosum. They report that species with larger
11 brains have relatively small corpus callosi, suggesting that humans have increasingly “split” or
12 “disconnected” hemispheres, followed by great apes, then Old World monkeys. Nevertheless,
13 as the present and previous studies have shown (Xiang et al., 2018; Xiang et al., 2019a and b)
14 certain population level asymmetries are, however, unique to the human brain (Crow, 2004;
15 Crow, 2010). We believe that the common ancestor of humans and great apes had already
16 present cortical asymmetry, most likely in the peri-Sylvian region, such as leftward SA
17 asymmetry in PT. After the separation from the common ancestor, brain asymmetry appears to
18 have developed independently in individual species, influenced by both genetic and
19 environmental factors. The new and more extensive asymmetries of the medial occipital lobe
20 and STS in the human brain are more likely to be related to the lateralization in cognitive
21 abilities, such as left hemisphere dominance for language.
22
23
24
25
26
27
28
29
30
31
32
33
34
35

36 The failure to detect a significant correlation between SA and CT asymmetry in either
37 species is consistent with the previous studies in humans (Winkler et al. 2010) and chimpanzees
38 (Hopkins & Avants, 2013), supporting that SA and CT have developmental phenotypes that
39 are presumably dependent upon different factors (Panizzon et al., 2009; Winkler et al., 2010).
40 Albeit, interestingly, a marginally significant correlation was observed between asymmetries
41 of the human and chimpanzee brain in CT ($p = 0.05$), but not SA. This finding suggests that
42 the human brain can be better distinguished from the chimpanzee brain on the basis of SA
43 rather than CT asymmetry, which is in line with the claim that more substantial change existing
44 in SA than CT during the course of human evolution (Lyall et al., 2015; Meyer, Liem, Hirsiger,
45 Jancke, & Hanggi, 2014; Rakic, 1995), and it is also relevant to another observation that general
46 cognitive ability is driven by SA rather than CT (Vuoksimaa et al. 2015). In this context, our
47 result points out that the search for neural structural basis underlying superior human cognitive
48 ability in comparative studies should be more fruitful if it is based on SA.
49
50
51
52
53
54
55
56
57
58
59
60

1
2
3
4
5
6
7
8
9
10
11
12
13
14
15
16
17
18
19
20
21
22
23
24
25
26
27
28
29
30
31
32
33
34
35
36
37
38
39
40
41
42
43
44
45
46
47
48
49
50
51
52
53
54
55
56
57
58
59
60

There is no significant sex effect on brain SA or CT at the global level for either species. However, an interesting sexual dimorphism of SA asymmetry is observed in the superior temporal lobe in the human brain. In particular, males were found to be significantly more leftward asymmetric in this brain region than females ($p < 0.001$). The sex difference was significant ($p = 0.003$), though did not survive Bonferroni correction for multiple comparisons. Kong et al. (2018), also reported a sex difference in the same region in investigating a larger cohort of healthy subjects. In an aneuploidy study, based on the observation of more pronounced asymmetry in XY males than XX females and XXY males within the superior temporal lobe, Savic (2014) raised the possibility that the associated region to be responsible for the sex difference that has been widely reported in speech processing.

A limitation of the study is that the gyral boundaries used for parcellation of the chimpanzee brain are derived from the Desikan-Killiany neuro-anatomical atlas of the human brain (Desikan et al., 2006) which was constructed by averaging boundaries manually delineated for 34 ROIs on the basis of relevant gyri in each cerebral hemisphere of co-registered 3D MRI scans obtained for 40 individuals. In several previous studies the brains of individual subjects in human and chimpanzee cohorts have been co-registered to a common reference space using the FreeSurfer pipeline (Xiang et al., 2018; Xiang et al., 2019a and b) and in one study the Desikan-Killiany atlas was applied to compare corresponding ROIs in the human and chimpanzee brain (Hopkins et al., 2017). In each case the co-registration using FreeSurfer is checked by using rigorous quality control procedures (Xiang et al. 2018) and the subsequent use of the Desikan-Killiany atlas is possible because the average pattern of the primary, and many of the secondary and tertiary gyri, is closely similar in the human and chimpanzee brain. Thus although within the 34 ROIs in each cerebral hemisphere there are undoubtedly variations in the gyral pattern, as shown in Figure S3 of Supplementary Materials the bounding gyri show close correspondence between the human and chimpanzee brain. Besides, the SAPS-based regional result is highly consistent with the vertex-wise result that is less prone to the above mentioned atlas-bias. In an alternative approach to atlas-based ROI analysis, Le Guen et al. (2018a; 2018b) proposed a novel strategy. In particular, the location of sulcal pits in the left and right cerebral hemispheres of individual subjects is determined and then a watershed algorithm is applied to define mutual boundaries for new ROIs in each cerebral hemispheres. The method essentially generates a study-specific symmetric parcellation standard for subsequent regional analysis and is likely to be widely employed in future studies. The approach is not, however, as suitable for use in the present comparative study as it is unlikely that the two species share the same pattern of distribution of sulcal pits. Another limitation is

1
2
3 the lack of investigation of handedness effect on brain asymmetries, which was infeasible
4 because of the incompleteness of handedness information for the human cohort. Although, as
5 mentioned before, no significant association between brain asymmetries and handedness was
6 detected for any of the ROI's in the meta-analysis performed by Kong et al. (2018) (see also
7 the vertex-wise SA and CT asymmetry analysis reported by Maingault et al. (2016)). It should
8 also be emphasised that inconsistencies with results reported in other studies could be related
9 to (i) methodological differences such as use of SAPS compared to TAPS, use of SBM rather
10 than VBM and use of automatic compared to manual methods (e.g. automatic parcellation
11 versus manual outlining of ROIs), (ii) spatial resolution (e.g. 163,842 vertices per cerebral
12 hemisphere in the present study compared to 40,962 vertices per cerebral hemisphere in the
13 study by (Zhou et al., 2013)), (iii) statistical methods, (iv) *in-vivo* versus *in-vitro* studies and
14 (v) sample size considerations.

15
16
17
18
19
20
21
22
23
24 In summary, we have presented the most comprehensive comparison so far available
25 for SA and CT asymmetry between the human and chimpanzee brain. Overall, the human brain
26 shows much greater asymmetry with distinct global and local features, whereas the chimpanzee
27 brain is comparatively less asymmetric with seemingly only local asymmetries being present
28 rather than having a global pattern of asymmetry such as the torque. The species difference is
29 qualitative rather than quantitative. In most regions where present significant difference
30 between the human and chimpanzee brain, the sign of the average brain asymmetry is in
31 opposite direction. Thus, it is probably not true that the two species share the same asymmetry
32 but which is only more prominent in humans (Gomez-Robles et al., 2013).

33
34
35
36
37
38
39
40 With regard to local asymmetries that are present in the human and chimpanzee brain,
41 there is diminishing evidence for the one that was long predicted and expected to be found in
42 Broca's area and its homologue, but on the other hand increasing evidence that both species
43 share a common leftward asymmetry in PT and its homologue. Accordingly, against the
44 backdrop of a global torque present in only the human brain is the interesting finding that the
45 two species likely share an identical pattern of presence, and absence, of structural asymmetries
46 in receptive, and expressive, "language" areas. Added to this are intriguing findings of
47 structural asymmetries unique to each species, namely we found further support for the
48 rightward STS asymmetry proposed by Leroy et al. (2015) to be a human-specific landmark
49 and observed for the first time a chimpanzee-specific asymmetry of the precentral gyrus and
50 which could possibly provide information relevant to deciphering the brain changes that may
51 have occurred related to the evolution of handedness.

1
2
3 In conclusion, after being highly sought after for well over a century but remaining
4 somewhat enigmatic, a clearer picture is finally emerging regarding the nature of structural
5 brain asymmetry and its evolution and many interesting lines of enquiry can now be more
6 confidently pursued. The above mentioned asymmetries are all relatively subtle, but they are
7 real, and they may be measured in unprecedented detail by using state of the art MR imaging
8 and image analysis techniques such as those used in the present study and which are becoming
9 ever more refined and sophisticated. Coupled with advances in genetics, “Big Data” and
10 artificial intelligence we anticipate the study of structural brain asymmetries is poised to lead
11 to new knowledge and new understanding regarding brain evolution and brain structural and
12 functional organisation and we hope that the findings of the present study will provide further
13 motivation to conduct these analyses.
14
15
16
17
18
19
20
21
22
23
24
25
26
27
28
29
30
31
32
33
34
35
36
37
38
39
40
41
42
43
44
45
46
47
48
49
50
51
52
53
54
55
56
57
58
59
60

Acknowledgments

LX was supported by T.J. Crow Psychosis Research Trust and WDH was supported by NIH grant NS-42867 and HD-60563. We thank Prof. Stephen Lawrie for access to MRI scans of human subjects at the University of Edinburgh and staff at the University of Edinburgh, University of Oxford and Yerkes National Primate Center for their support in acquiring the MRI data.

For Peer Review

References

- Amunts K, Schlaug G, Schleicher A, Steinmetz H, Dabringhaus A, Roland PE, Zilles K. 1996. Asymmetry in the human motor cortex and handedness. *Neuroimage*. 4(3 Pt 1):216-222.
- Balzeau A, Gilissen E. 2010. Endocranial shape asymmetries in *pan paniscus*, *pan troglodytes* and gorilla gorilla assessed via skull based landmark analysis. *J Hum Evol*. 59:54-69.
- Balzeau A, Gilissen E, Grimaud-Herve D. 2012. Shared pattern of endocranial shape asymmetries among great apes, anatomically modern humans, and fossil hominins. *PLoS One*. 7(1):e29581.
- Cantalupo C, Hopkins WD. 2001. Asymmetric Broca's area in great apes. *Nature*. 414(6863):505.
- Chiarello C, Vazquez D, Felton A, McDowell A. 2016. Structural asymmetry of the human cerebral cortex: Regional and between-subject variability of surface area, cortical thickness, and local gyrification. *Neuropsychologia*. 93(Pt B):365-379.
- Corballis M. 2004. Laterality and human speciation. *Proceedings of the British Academy*. p: 136-152.
- Crow T. 2004. Directional asymmetry is the key to the origin of modern *homo sapiens* (the Broca-Annett axiom): A reply to Rogers' review of the speciation of modern *homo sapiens*. *Laterality: Asymmetries of Body, Brain and Cognition*. 9:233-242.
- Crow TJ. 2010. A theory of the origin of cerebral asymmetry: Epigenetic variation superimposed on a fixed right-shift. *Laterality*. 15:289-303.
- Cunningham DJ. 1892. Contribution to the surface anatomy of the cerebral hemispheres. *Cunningham Mem (R Ir Acad)*. 7(372).
- Dale AM, Fischl B, Sereno, M.I. 1999. Cortical surface-based analysis I: Segmentation and surface reconstruction. *NeuroImage*. 9:179-194.
- Desikan RS, Segonne F, Fischl B, Quinn BT, Dickerson BC, Blacker D, Buckner RL, Dale AM, Maguire RP, Hyman BT et al. 2006. An automated labeling system for subdividing the human cerebral cortex on MRI scans into gyral based regions of interest. *Neuroimage*. 31:968-980.
- Destrieux C, Fischl B, Dale A, Halgren E. 2010. Automatic parcellation of human cortical gyri and sulci using standard anatomical nomenclature. *Neuroimage*. 53:1-15.
- Eberstaller O. 1884. Zür oberflachen anatomie der grosshirn hemisphaeren. *Wien Med*. 7(479):642-644.

- 1
2
3 Eberstaller O. 1890. Das stirnhirn. Ein beitrage zur anatomie der oberfläche des grosshirns.
4 Urban and schwarzenberg, wien und leipzig.
5
6 Foundas AL, Eure KF, Luevano LF, Weinberger DR. 1998. MRI asymmetries of Broca's area:
7 The pars triangularis and pars opercularis. *Brain Lang.* 64(3):282-296.
8
9 Gannon PJ, Holloway RL, Broadfield DC, Braun AR. 1998. Asymmetry of chimpanzee
10 planum temporale: Humanlike pattern of Wernicke's brain language area homolog.
11 *Science.* 279(5348):220-222.
12
13 Geschwind N, Levitsky W. 1968. Human brain: Left-right asymmetries in temporal speech
14 region. *Science.* 161(3837):186-187.
15
16 Gomez-Robles A, Hopkins WD, Sherwood CC. 2013. Increased morphological asymmetry,
17 evolvability and plasticity in human brain evolution. *Proc Biol Sci.*
18 280(1761):20130575.
19
20 Good CD, Johnsrude I, Ashburner J, Henson RN, Friston KJ, Frackowiak RS. 2001. Cerebral
21 asymmetry and the effects of sex and handedness on brain structure: A voxel-based
22 morphometric analysis of 465 normal adult human brains. *Neuroimage.* 14(3):685-700.
23
24 Greve DN, Van der Haegen L, Cai Q, Stufflebeam S, Sabuncu MR, Fischl B, Brysbaert M.
25 2013. A surface-based analysis of language lateralization and cortical asymmetry. *J*
26 *Cogn Neurosci.* 25(9):1477-1492.
27
28 Hopkins WD. 1995. Hand preferences for a coordinated bimanual task in 110 chimpanzees
29 (*pan troglodytes*): Cross-sectional analysis. *J Comp Psychol.* 109(3):291-297.
30
31 Hopkins WD. 2013. Neuroanatomical asymmetries and handedness in chimpanzees (*pan*
32 *troglodytes*): A case for continuity in the evolution of hemispheric specialization. *Ann*
33 *N Y Acad Sci.* 1288:17-35.
34
35 Hopkins WD, Avants BB. 2013. Regional and hemispheric variation in cortical thickness in
36 chimpanzees (*pan troglodytes*). *J Neurosci.* 33(12):5241-5248.
37
38 Hopkins WD, Cantalupo C. 2004. Handedness in chimpanzees (*pan troglodytes*) is associated
39 with asymmetries of the primary motor cortex but not with homologous language areas.
40 *Behav Neurosci.* 118(6):1176-1183.
41
42 Hopkins WD, Li X, Crow T, Roberts N. 2016. Vertex- and atlas-based comparisons in
43 measures of cortical thickness, gyrification and white matter volume between humans
44 and chimpanzees. *Brain Struct Funct.* 222(1):229-245.
45
46 Hopkins WD, Meguerditchian A, Coulon O, Bogart S, Mangin JF, Sherwood CC, Grabowski
47 MW, Bennett AJ, Pierre PJ, Fears S et al. 2014. Evolution of the central sulcus
48 morphology in primates. *Brain Behav Evol.* 84(1):19-30.
49
50
51
52
53
54
55
56
57
58
59
60

- 1
2
3 Hopkins WD, Nir TM. 2010. Planum temporale surface area and grey matter asymmetries in
4 chimpanzees (*pan troglodytes*): The effect of handedness and comparison with findings
5 in humans. *Behav Brain Res.* 208(2):436-443.
6
7
8 Hopkins WD, Tagliabue JP, Meguerditchian A, Nir T, Schenker NM, Sherwood CC. 2008.
9 Grey matter asymmetries in chimpanzees as revealed by voxel-based morphometry.
10 *Neuroimage.* 42(2):491-497.
11
12
13 Hou L, Xiang L, Crow T, Leroy F, Riviere D, Mangin JF, Roberts N. 2018. Measurement of
14 Sylvian Fissure asymmetry and occipital bending in humans and *pan troglodytes*.
15 *Neuroimage.* 184:855-870.
16
17
18 Keller SS, Crow T, Foundas A, Amunts K, Roberts N. 2009a. Broca's area: Nomenclature,
19 anatomy, typology and asymmetry. *Brain Lang.* 109(1):29-48.
20
21
22 Keller SS, Deppe M, Herbin M, Gilissen E. 2012. Variability and asymmetry of the sulcal
23 contours defining Broca's area homologue in the chimpanzee brain. *J Comp Neurol.*
24 520(6):1165-1180.
25
26
27 Keller SS, Roberts N, Hopkins W. 2009b. A comparative magnetic resonance imaging study
28 of the anatomy, variability, and asymmetry of Broca's area in the human and
29 chimpanzee brain. *J Neurosci.* 29(46):14607-14616.
30
31
32 Koelkebeck K, Miyata J, Kubota M, Kohl W, Son S, Fukuyama H, Sawamoto N, Takahashi
33 H, Murai T. 2014. The contribution of cortical thickness and surface area to grey matter
34 asymmetries in the healthy human brain. *Hum Brain Mapp.* 35(12):6011-6022.
35
36
37 Kong XZ, Mathias SR, Guadalupe T, Glahn DC, Franke B, Crivello F, Tzourio-Mazoyer N,
38 Fisher SE, Thompson PM, Francks C. 2018. Mapping cortical brain asymmetry in
39 17,141 healthy individuals worldwide via the enigma consortium. *Proc Natl Acad Sci*
40 *U S A.* 115(22):E5154-e5163.
41
42
43 LeMay M. 1976. Morphological cerebral asymmetries of modern man, fossil man, and
44 nonhuman primate. *Ann N Y Acad Sci.* 280:349-366.
45
46
47 LeMay M, Billig MS, Geschwind N. 1982. Asymmetries of the brains and skulls of nonhuman
48 primates. In: E. Armstrong DF, editor. *Primate brain evolution methods and concepts.*
49 New York: Plenum Press. p:263-277.
50
51
52
53 Leroy F, Cai Q, Bogart SL, Dubois J, Coulon O, Monzalvo K, Fischer C, Glasel H, Van der
54 Haegen L, Benezit A et al. 2015. New human-specific brain landmark: The depth
55 asymmetry of superior temporal sulcus. *Proc Natl Acad Sci U S A.* 112(4):1208-1213.
56
57
58 Luders E, Narr KL, Thompson PM, Rex DE, Jancke L, Toga AW. 2006. Hemispheric
59 asymmetries in cortical thickness. *Cereb Cortex.* 16(8):1232-1238.
60

- 1
2
3 Lyall AE, Shi F, Geng X, Woolson S, Li G, Wang L, Hamer RM, Shen D, Gilmore JH. 2015.
4
5 Dynamic development of regional cortical thickness and surface area in early childhood.
6
7 Cereb Cortex. 25(8):2204-2212.
- 8
9 Lyn H, Pierre P, Bennett AJ, Fears S, Woods R, Hopkins WD. 2011. Planum temporale grey
10
11 matter asymmetries in chimpanzees (*pan troglodytes*), vervet (*chlorocebus aethiops*
12
13 *sabaeus*), rhesus (*macaca mulatta*) and bonnet (*macaca radiata*) monkeys.
14
15 Neuropsychologia. 49(7):2004-2012.
- 16
17 Lyttelton OC, Karama S, Ad-Dab'bagh Y, Zatorre RJ, Carbonell F, Worsley K, Evans AC.
18
19 2009. Positional and surface area asymmetry of the human cerebral cortex. Neuroimage.
20
21 46(4):895-903.
- 22
23 Maingault S, Tzourio-Mazoyer N, Mazoyer B, Crivello F. 2016. Regional correlations between
24
25 cortical thickness and surface area asymmetries: A surface-based morphometry study
26
27 of 250 adults. Neuropsychologia. 93(Pt B):350-364.
- 28
29 Meyer M, Liem F, Hirsiger S, Jancke L, Hanggi J. 2014. Cortical surface area and cortical
30
31 thickness demonstrate differential structural asymmetry in auditory-related areas of the
32
33 human cortex. Cereb Cortex. 24(10):2541-2552.
- 34
35 Balzeau, A., & Gilissen, E. (2010). Endocranial shape asymmetries in *Pan paniscus*, *Pan*
36
37 *troglodytes*, and *Gorilla gorilla* assessed via skull based landmark analysis. Journal of
38
39 Human Evolution, 59, 54-69.
- 40
41 Barrick, T. R., Lawes, N., Mackay, C. E., & Clark, C. A. (2007). White matter pathway
42
43 asymmetry underlies functional lateralization. Cerebral Cortex, 17(3), 591-598.
- 44
45 Bradshaw, B., & Rogers, L. (1993). The evolution of lateral asymmetries, language, tool-use
46
47 and intellect. San Diego: Academic Press.
- 48
49 Cantalupo, C., & Hopkins, W. D. (2001). Asymmetric Broca's area in great apes. Nature,
50
51 414(6863), 505. doi:10.1038/35107134
- 52
53 Chiarello, C., Vazquez, D., Felton, A., & McDowell, A. (2016). Structural asymmetry of the
54
55 human cerebral cortex: Regional and between-subject variability of surface area,
56
57 cortical thickness, and local gyrification. Neuropsychologia, 93(Pt B), 365-379.
58
59 doi:10.1016/j.neuropsychologia.2016.01.012
- 60
61 Corballis, M. C. (1992). The lopsided brain: Evolution of the generative mind. New York:
62
63 Oxford University Press.
- 64
65 Corballis, M. C. (2002). From hand to mouth: The origins of language. Princeton, NJ: Princeton
66
67 University Press.

- 1
2
3 Corballis, M. C. (2009). The evolution and genetics of cerebral asymmetry. *Philos Trans R Soc*
4 *Lond B Biol Sci*, 364(1519), 867-879. doi:10.1098/rstb.2008.0232
- 5
6 Crow, T. J. (2009). A theory of the origin of cerebral asymmetry: Epigenetic variation
7 superimposed on a fixed right-shift. *Laterality*, 15(3), 289-303.
- 8
9
10 Cunningham, D. J. (1892). Contribution to the surface anatomy of the cerebral hemispheres.
11 *Cunningham Mem. (R. Ir. Acad.)*, 7(372).
- 12
13 Dale, A. M., Fischl, B., Sereno, M.I. (1999). Cortical Surface-Based Analysis I: Segmentation
14 and Surface Reconstruction. *NeuroImage*, 9(2), 179-194
- 15
16
17 Desikan, R. S., Segonne, F., Fischl, B., Quinn, B. T., Dickerson, B. C., Blacker, D., Killiany,
18 R. J. (2006). An automated labeling system for subdividing the human cerebral cortex
19 on MRI scans into gyral based regions of interest. *Neuroimage*, 31(3), 968-980.
20 doi:10.1016/j.neuroimage.2006.01.021
- 21
22
23 Eberstaller, O. (1884). Zür Oberflächen Anatomie der Grosshirn Hemisphaeren *Wien Med*,
24 7(479), 642-644.
- 25
26
27 Eberstaller, O. (1890). Das Stirnhirn. Ein Beitrag zur Anatomie der Oberfläche des Grosshirns.
28 Urban & Schwarzenberg, Wien und Leipzig.
- 29
30
31 Fischl, B., Sereno, M. I., Tootell, R. B., & Dale, A. M. (1999). High-resolution intersubject
32 averaging and a coordinate system for the cortical surface. *Hum Brain Mapp*, 8(4), 272-
33 284. doi:10.1002/(sici)1097-0193(1999)8:4<272::aid-hbm10>3.0.co;2-4
- 34
35
36 Gannon, P. J., Holloway, R. L., Broadfield, D. C., & Braun, A. R. (1998). Asymmetry of
37 chimpanzee Planum Temporale: Humanlike pattern of Wernicke's language area
38 homolog. *Science*, 279, 220-222.
- 39
40
41 Gannon, P. J., Kheck, N., & Hof, P. R. (2008). Leftward interhemispheric asymmetry of
42 macaque monkey temporal lobe language area homolog is evident at the
43 cytoarchitectural, but not gross anatomic level. *Brain Research*, 1199, 62-73.
- 44
45
46 Geschwind, N., & Levitsky, W. (1968). Human brain: left-right asymmetries in temporal
47 speech region. *Science*, 161(3837), 186-187.
- 48
49
50 Gomez-Robles, A., Hopkins, W. D., & Sherwood, C. C. (2013). Increased morphological
51 asymmetry, evolvability and plasticity in human brain evolution. *Proc Biol Sci*,
52 280(1761), 20130575. doi:10.1098/rspb.2013.0575
- 53
54
55 Good, C. D., Johnsrude, I., Ashburner, J., Henson, R. N., Friston, K. J., & Frackowiak, R. S.
56 (2001). Cerebral asymmetry and the effects of sex and handedness on brain structure:
57 a voxel-based morphometric analysis of 465 normal adult human brains. *Neuroimage*,
58 14(3), 685-700. doi:10.1006/nimg.2001.0857
- 59
60

- 1
2
3 Greve, D. N., Van der Haegen, L., Cai, Q., Stufflebeam, S., Sabuncu, M. R., Fischl, B., &
4 Brysbaert, M. (2013). A surface-based analysis of language lateralization and cortical
5 asymmetry. *J Cogn Neurosci*, 25(9), 1477-1492. doi:10.1162/jocn_a_00405
6
7
8 Guadalupe, T., Willems, R. M., Zwiers, M. P., Arias Vasquez, A., Hoogman, M., Hagoort, P.,
9 Francks, C. (2014). Differences in cerebral cortical anatomy of left- and right-handers.
10 *Front Psychol*, 5, 261. doi:10.3389/fpsyg.2014.00261
11
12
13 Holloway, R. L., & De La Costelareymondie, M. C. (1982). Brain endocast asymmetry in
14 pongids and hominids: some preliminary findings on the paleontology of cerebral
15 dominance. *Am J Phys Anthropol*, 58(1), 101-110. doi:10.1002/ajpa.1330580111
16
17
18 Hopkins, W. D., & Avants, B. B. (2013). Regional and hemispheric variation in cortical
19 thickness in chimpanzees (*Pan troglodytes*). *J Neurosci*, 33(12), 5241-5248.
20 doi:10.1523/jneurosci.2996-12.2013
21
22
23 Hopkins, W. D., & Cantalupo, C. (2004). Handedness in chimpanzees (*Pan troglodytes*) is
24 associated with asymmetries of the primary motor cortex but not with homologous
25 language areas. *Behav Neurosci*, 118(6), 1176-1183. doi:10.1037/0735-
26 7044.118.6.1176
27
28
29 Hopkins, W. D., Li, X., Crow, T., & Roberts, N. (2016). Vertex- and atlas-based comparisons
30 in measures of cortical thickness, gyrification and white matter volume between
31 humans and chimpanzees. *Brain Struct Funct*. doi:10.1007/s00429-016-1213-1
32
33
34 Hopkins, W. D., & Marino, L. (2000). Asymmetries in cerebral width in nonhuman primate
35 brains as revealed by magnetic resonance imaging (MRI). *Neuropsychologia*, 38(4),
36 493-499.
37
38
39 Hopkins, W. D., Misiura, M., Pope, S. M., & Latash, E. M. (2015). Behavioral and brain
40 asymmetries in primates: a preliminary evaluation of two evolutionary hypotheses. *Ann*
41 *N Y Acad Sci*, 1359, 65-83. doi:10.1111/nyas.12936
42
43
44 Hopkins, W. D., & Nir, T. (2010). Planum temporale surface area and grey matter asymmetries
45 in chimpanzees (*Pan troglodytes*): The effect of handedness and comparison within
46 findings in humans. *Behavioural Brain Research*, 208(2), 436-443.
47
48
49 Ide, A., Rodriguez, E., Zaidel, E., & Aboitiz, F. (1996). Bifurcation patterns in the human
50 Sylvian fissure: hemispheric and sex differences. *Cerebral Cortex*, 6(5), 717-725.
51
52
53 Josse, G., Kherif, G., Flandin, G., Seghier, M. L., & Price, C. J. (2009). Predicting language
54 lateralization from gray matter. *Journal of Neuroscience*, 29(43), 13516-13523.
55
56
57
58
59
60

- 1
2
3 Keller, S. S., Deppe, M., Herbin, M., & Gilissen, E. (2012). Variability and asymmetry of the
4 sulcal contours defining Broca's area homologue in the chimpanzee brain. *J Comp*
5 *Neurol*, 520(6), 1165-1180. doi:10.1002/cne.22747
6
7
8 Keller, S. S., Highley, J. R., Garcia-Finana, M., Sluming, V., Rezaie, R., & Roberts, N. (2007).
9 Sulcal variability, stereological measurement and asymmetry of Broca's area on MR
10 images. *J Anat*, 211(4), 534-555. doi:10.1111/j.1469-7580.2007.00793.x
11
12
13 Knecht, S., Drager, B., Deppe, M., Bobe, L., Lohmann, H., Floel, A., Henningsen, H. (2000).
14 Handedness and hemispheric language dominance in healthy humans. *Brain*, 123(12),
15 2512-2518.
16
17
18 Koelkebeck, K., Miyata, J., Kubota, M., Kohl, W., Son, S., Fukuyama, H., Murai, T. (2014).
19 The contribution of cortical thickness and surface area to gray matter asymmetries in
20 the healthy human brain. *Hum Brain Mapp*, 35(12), 6011-6022.
21 doi:10.1002/hbm.22601
22
23
24 Kong, X. Z., Mathias, S. R., Guadalupe, T., Glahn, D. C., Franke, B., Crivello, F., Francks, C.
25 (2018). Mapping cortical brain asymmetry in 17,141 healthy individuals worldwide via
26 the ENIGMA Consortium. *Proc Natl Acad Sci U S A*, 115(22), E5154-e5163.
27 doi:10.1073/pnas.1718418115
28
29
30
31
32 Le Guen, Y., Auzias, G., Leroy, F., Noulhiane, M., Dehaene-Lambertz, G., Duchesnay, E.,
33 Frouin, V. (2018a). Genetic Influence on the Sulcal Pits: On the Origin of the First
34 Cortical Folds. *Cereb Cortex*, 28(6), 1922-1933. doi:10.1093/cercor/bhx098
35
36
37 Le Guen, Y., Leroy, F., Auzias, G., Riviere, D., Grigis, A., Mangin, J. F., Frouin, V. (2018b).
38 The chaotic morphology of the left superior temporal sulcus is genetically constrained.
39 *Neuroimage*, 174, 297-307. doi:10.1016/j.neuroimage.2018.03.046
40
41
42 LeMay, M. (1982). Morphological aspects of human brain asymmetry: An evolutionary
43 perspective. *Trends in Neurosciences*, 5, 273-275.
44
45
46 Leroy, F., Cai, Q., Bogart, S. L., Dubois, J., Coulon, O., Monzalvo, K., Dehaene-Lambertz, G.
47 (2015). New human-specific brain landmark: the depth asymmetry of superior temporal
48 sulcus. *Proc Natl Acad Sci U S A*, 112(4), 1208-1213. doi:10.1073/pnas.1412389112
49
50
51 Luders, E., Narr, K. L., Thompson, P. M., Rex, D. E., Jancke, L., & Toga, A. W. (2006).
52 Hemispheric asymmetries in cortical thickness. *Cereb Cortex*, 16(8), 1232-1238.
53 doi:10.1093/cercor/bhj064
54
55
56 Lyall, A. E., Shi, F., Geng, X., Woolson, S., Li, G., Wang, L., Gilmore, J. H. (2015). Dynamic
57 Development of Regional Cortical Thickness and Surface Area in Early Childhood.
58 *Cereb Cortex*, 25(8), 2204-2212. doi:10.1093/cercor/bhu027
59
60

- 1
2
3 Lyn, H. L., Pierre, P., Bennett, A. J., Fears, S. C., Woods, R. P., & Hopkins, W. D. (2011).
4 Planum temporale grey matter asymmetries in chimpanzees (*Pan troglodytes*), vervet
5 (*Chlorocebus aethiops sabaeus*), rhesus (*Macaca mulatta*) and bonnet (*Macaca radiata*)
6 monkeys. *Neuropsychologia*, 49, 2004-2012.
7
8
9
10 Lyttelton, O. C., Karama, S., Ad-Dab'bagh, Y., Zatorre, R. J., Carbonell, F., Worsley, K., &
11 Evans, A. C. (2009). Positional and surface area asymmetry of the human cerebral
12 cortex. *Neuroimage*, 46(4), 895-903. doi:10.1016/j.neuroimage.2009.03.063
13
14
15 Maingault, S., Tzourio-Mazoyer, N., Mazoyer, B., & Crivello, F. (2016). Regional correlations
16 between cortical thickness and surface area asymmetries: A surface-based
17 morphometry study of 250 adults. *Neuropsychologia*, 93(Pt B), 350-364.
18 doi:10.1016/j.neuropsychologia.2016.03.025
19
20
21
22 Marie, D., Roth, M., Lacoste, R., Nazarian, B., Bertello, A., Anton, J. L., Meguerditchian, A.
23 (2017). Left Brain Asymmetry of the Planum Temporale in a Nonhominid Primate:
24 Redefining the Origin of Brain Specialization for Language. *Cereb Cortex*, 1-8.
25 doi:10.1093/cercor/bhx096
26
27
28
29 Meyer, M., Liem, F., Hirsiger, S., Jancke, L., & Hanggi, J. (2014). Cortical surface area and
30 cortical thickness demonstrate differential structural asymmetry in auditory-related
31 areas of the human cortex. *Cereb Cortex*, 24(10), 2541-2552.
32 doi:10.1093/cercor/bht094
33
34
35
36 Ocklenburg, S., & Gunturkun, O. (2018). *The Lateralized Brain: The Neuroscience and*
37 *Evolution of Hemispheric Asymmetries*. London: Academic Press.
38
39
40 Panizzon, M. S., Fennema-Notestine, C., Eyler, L. T., Jernigan, T. L., Prom-Wormley, E.,
41 Neale, M., Kremen, W. S. (2009). Distinct genetic influences on cortical surface area
42 and cortical thickness. *Cereb Cortex*, 19(11), 2728-2735. doi:10.1093/cercor/bhp026
43
44
45 Plessen, K. J., Hugdahl, K., Bansal, R., Hao, X., & Peterson, B. S. (2014). Sex, age, and
46 cognitive correlates of asymmetries in thickness of the cortical mantle across the life
47 span. *J Neurosci*, 34(18), 6294-6302. doi:10.1523/jneurosci.3692-13.2014
48
49
50 Rakic, P. (1995). A small step for the cell, a giant leap for mankind: a hypothesis of neocortical
51 expansion during evolution. *Trends Neurosci*, 18(9), 383-388.
52
53
54 Rilling, J. K., Glasser, M. F., Jbabdi, S., Andersson, J., & Preuss, T. M. (2011). Continuity,
55 divergence, and the evolution of brain language pathways. *Front Evol Neurosci*, 3, 11.
56 doi:10.3389/fnevo.2011.00011
57
58
59 Rogers, L. J., Vallortigara, G., & Andrew, R. J. (2013). *Divided brains: the biology and*
60 *behaviour of brain asymmetries*. New York: Cambridge University Press.

- 1
2
3 Rubens, A. B., Mahowald, M. W., & Hutton, J. T. (1976). Asymmetry of the lateral (Sylvian)
4 fissures in man. *Neurology*, 26(7), 620-624.
5
6 Savic, I. (2014). Asymmetry of cerebral gray and white matter and structural volumes in
7 relation to sex hormones and chromosomes. *Front Neurosci*, 8, 329.
8 doi:10.3389/fnins.2014.00329
9
10 Shapleske, J., Rossell, S. L., Woodruff, P. W., & David, A. S. (1999). The planum temporale:
11 a systematic, quantitative review of its structural, functional and clinical significance.
12 *Brain Research Reviews*, 29, 26-49.
13
14 Sherwood, C. C., Wahl, E., Erwin, J. M., Hof, P. R., & Hopkins, W. D. (2007). Histological
15 asymmetries of primary motor cortex predict handedness in chimpanzees (*Pan*
16 *troglodytes*). *J Comp Neurol*, 503(4), 525-537. doi:10.1002/cne.21399
17
18 Takaya, S., Kuperberg, G. R., Liu, H., Greve, D. N., Makris, N., & Stufflebeam, S. M. (2015).
19 Asymmetric projections of the arcuate fasciculus to the temporal cortex underlie
20 lateralized language function in the human brain. *Front Neuroanat*, 9, 119.
21 doi:10.3389/fnana.2015.00119
22
23 Trivedi, R., Agarwal, S., Rathore, R. K., Saksena, S., Tripathi, R. P., Malik, G. K., Gupta, R.
24 K. (2009). Understanding development and lateralization of major cerebral fiber
25 bundles in pediatric population through quantitative diffusion tensor tractography.
26 *Pediatr Res*, 66(6), 636-641. doi:10.1203/PDR.0b013e3181bbc6b5
27
28 Vadlamudi, L., Hatton, R., Byth, K., Harasty, J., Vogrin, S., Cook, M. J., & Bleasel, A. F.
29 (2006). Volumetric analysis of a specific language region- the planum temporale.
30 *Journal of Clinical Neuroscience*, 13, 206-213.
31
32 Van Essen, D. C., Glasser, M. F., Dierker, D. L., Harwell, J., & Coalson, T. (2012).
33 Parcellations and hemispheric asymmetries of human cerebral cortex analyzed on
34 surface-based atlases. *Cereb Cortex*, 22(10), 2241-2262. doi:10.1093/cercor/bhr291
35
36 Vuoksimaa E, Panizzon MS, Chen CH, Fiecas M, Eyler LT, Fennema-Notestine C, Hagler DJ,
37 Fischl B, Franz CE, Jak A et al. 2015. The genetic association between neocortical
38 volume and general cognitive ability is driven by global surface area rather than
39 thickness. *Cereb Cortex*. 25(8):2127-2137.
40
41 Watkins, K. E., Paus, T., Lerch, J. P., Zijdenbos, A., Collins, D. L., Neelin, P., Taylor, J.,
42 Worsley, K. J., Evans, A. C. 2001. Structural asymmetries in the human brain: A voxel-
43 based statistical analysis of 142 MRI scans. *Cereb Cortex*. 11(9):868-877.
44
45
46
47
48
49
50
51
52
53
54
55
56
57
58
59
60

- 1
2
3
4
5
6
7
8
9
10
11
12
13
14
15
16
17
18
19
20
21
22
23
24
25
26
27
28
29
30
31
32
33
34
35
36
37
38
39
40
41
42
43
44
45
46
47
48
49
50
51
52
53
54
55
56
57
58
59
60
- Wiberg, A., Ng, M., Al Omran, Y., Alfaro-Almagro, F., McCarthy, P., Marchini, J., Furniss, D. (2019). Handedness, language areas and neuropsychiatric diseases: insights from brain imaging and genetics. *Brain*, 142(10), 2938-2947. doi:10.1093/brain/awz257
- Winkler, A. M., Kochunov, P., Blangero, J., Almasy, L., Zilles, K., Fox, P. T., Glahn, D. C. (2010). Cortical thickness or grey matter volume? The importance of selecting the phenotype for imaging genetics studies. *Neuroimage*, 53(3), 1135-1146. doi:10.1016/j.neuroimage.2009.12.028
- Witelson, S., & Kigar, D. (1988). Asymmetry of brain function follows asymmetry in anatomical form: gross, microscopic, postmortem and imaging studies. In: Boller, Grafman, J. (Eds.), *Handbook of Neuropsychology* (pp. 111–142): Elsevier.
- Xiang, L., Crow, T., & Roberts, N. (2019a). Automatic analysis of cross-sectional cerebral asymmetry on 3D in vivo MRI scans of human and chimpanzee. *J Neurosci Res*. doi:10.1002/jnr.24391
- Xiang, L., Crow, T., & Roberts, N. (2019b). Cerebral torque is human specific and unrelated to brain size. *Brain Struct Funct*. doi:10.1007/s00429-018-01818-0
- Xiang, L., Crow, T. J., Hopkins, W. D., Gong, Q., & Roberts, N. (2018). Human torque is not present in chimpanzee brain. *Neuroimage*, 165, 285-293. doi:10.1016/j.neuroimage.2017.10.017
- Yeni-Komshian, G., & Benson, D. (1976). Anatomical study of cerebral asymmetry in the temporal lobe of humans, chimpanzees and monkeys. *Science*, 192, 387-389.
- Zhou, D., Lebel, C., Evans, A., & Beaulieu, C. (2013). Cortical thickness asymmetry from childhood to older adulthood. *Neuroimage*, 83, 66-74. doi:10.1016/j.neuroimage.2013.06.073
- Zilles, K., Dabringhaus, A., Geyer, S., Amunts, K., Qu, M., Schleicher, A., Steinmetz, H. (1996). Structural asymmetries in the human forebrain and the forebrain of non-human primates and rats. *Neuroscience and Biobehavioral Reviews*, 20, 593-605.

Tables

	Methods and Measurements	Main findings of the study
Lyttelton et al. (2009), 112 right-handed human subjects	SBM-based vertex-wise analysis of SA and positional asymmetry	SA asymmetry to the left in the supra-marginal gyrus, Heschl's gyrus, PT, anterior superior temporal, lateral orbital frontal cortex and to the right in the anterior occipital lobe, dorsal anterior cingulate and medial orbital frontal; positional asymmetry in the pattern cerebral torque
Zhou et al. (2013), 274 right-handed human subjects	SBM-based vertex-wise analysis of CT asymmetry	CT asymmetry emerges extensively after adolescence and develops more pronounced with age
Maingault et al. (2016), 250 human subjects (120 left-handers)	SBM-based vertex-wise analysis of GMV, SA, CT and sulcal depth asymmetry	Global GMV, SA and CT asymmetry to the right; no significant correlation between the global SA and CT asymmetry; handedness is not associated with cortical asymmetries
Meyer et al. (2014), 104 healthy human subjects	Destrieux atlas-based ROI analysis of GMV, SA and CT asymmetry	Global rightward asymmetry in GMV and SA but not CT; leftward SA asymmetry in auditory-related cortex and rightward CT asymmetry in the primary and secondary auditory cortex
Koelkebeck et al. (2014), 101 right-handed human subjects	Desikan-Killiany atlas-based ROI analysis of GMV, SA and CT asymmetry	Different patterns of asymmetry in different measures; more prominent SA asymmetry compared to CT asymmetry
Chiarello et al. (2016), 200 healthy human subjects	Destrieux atlas-based ROI analysis of SA, CT and LGI asymmetry	Extensive asymmetries of all three measures; substantial differences between different measures in both pattern and extent; regions with larger between-subject variability also show greater asymmetry
Kong et al. (2018), 17,141 healthy human subjects	Desikan-Killiany atlas-based ROI analysis of SA, CT asymmetry	Global rightward asymmetry in SA and leftward asymmetry in CT; substantial and differential regional asymmetry in SA and CT which interacts with sex, age and ICV; no overall correlation between SA and CT asymmetry; handedness is not associated with cortical asymmetries
Guen et al. (2018b), 800+ subjects from the Human Connectome Project (HCP)	Novel ROI-based analysis of sulcal pit distribution asymmetry	Sulcal pit asymmetry in the STS to be genetically determined

Table 1. Studies of cerebral asymmetry in the human brain.

		Human		Chimpanzee	
Hemisphere		SA (x1.0e+05 mm ²)	CT (mm)	SA (x1.0e+04 mm ²)	CT (mm)
Left		1.11 ± 0.11	2.29 ± 0.09	3.67 ± 0.29	1.39 ± 0.11
Right		1.12 ± 0.11	2.30 ± 0.09	3.68 ± 0.29	1.40 ± 0.12
Asymmetry	t-stat	-3.82	-1.10	-0.39	-1.31
	p-value (2-tailed)	< 0.001	0.27	0.70	0.19

Table 2. Statistics of the global SA and CT values for the human and chimpanzee brain showing (i) significant rightward SA asymmetry in the human brain but not for CT, and (ii) no significant asymmetry for either SA or CT in the chimpanzee brain.

Surface Area ROIs	Human		Chimpanzee		Species Difference	
	AI	p-value	AI	p-value	t-stats	p-value
Frontal						
Superior frontal	-0.02	-0.03*	0.01	0.40	-2.14	0.03*
Rostral middle frontal	-0.02	-0.04*	-0.01	-0.46	-0.59	0.56
Caudal middle frontal	0.01	0.68	0.01	0.68	0.08	0.93
Pars-opercularis	0.01	0.51	0.00	0.90	0.41	0.68
Pars-triangularis	0.02	0.12	-0.00	-0.85	1.04	0.30
Pars-orbitalis	0.01	0.32	-0.02	-0.45	1.17	0.24
Lateral orbito frontal	0.01	0.13	0.03	0.10	-1.06	0.29
Medial orbito frontal	-0.09	-0.00**	0.01	0.78	-2.81	0.01*
Precentral	-0.01	-0.06	-0.01	-0.15	-0.58	0.56
Paracentral	0.01	0.36	-0.02	-0.02*	1.72	0.09
Frontal pole	-0.02	-0.13	0.00	0.83	-1.28	0.20
Parietal						
Superior parietal	-0.03	-0.002*	0.01	0.37	-2.91	0.00*
Inferior parietal	-0.05	-0.00**	-0.00	-0.79	-3.80	0.00**
Supramarginal	0.10	0.00**	0.01	0.10	5.47	0.00**
Postcentral	0.03	0.00**	-0.00	-0.68	3.25	0.00**
Precuneus	-0.01	-0.16	-0.01	-0.51	-0.30	0.76
Temporal						
Middle temporal	-0.00	-0.58	0.01	0.39	-1.03	0.30
Inferior temporal	0.04	0.00**	0.01	0.31	1.86	0.06
Superior temporal	0.02	0.03*	0.03	0.00**	-1.68	0.10
Bankssts	-0.05	-0.02*	-0.01	-0.17	-1.43	0.15
Fusiform	-0.00	-0.97	0.01	0.34	-0.81	0.42
Transverse temporal	0.07	0.00**	0.02	0.04*	2.53	0.01*
Entorhinal	-0.02	-0.23	-0.06	-0.13	0.83	0.41
Temporal pole	0.07	0.00**	0.02	0.37	1.93	0.05
Parahippocampal	-0.00	-0.96	-0.02	-0.50	0.61	0.54
Occipital						
Lateral occipital	-0.01	-0.24	-0.02	-0.08	0.53	0.60
Lingual	-0.03	-0.01*	-0.00	-0.88	-1.35	0.18
Cuneus	-0.09	-0.00**	0.08	0.00**	-7.04	0.00**
Pericalcarine	-0.06	-0.00**	0.00	0.99	-2.27	0.02*
Cingulate & Insula						
Caudal anterior cingulate	-0.09	-0.003*	0.05	0.02*	-3.69	0.00**
Isthmus cingulate	0.07	0.00**	-0.00	-0.99	2.16	0.03*
Posterior cingulate	-0.03	-0.02*	0.01	0.70	-1.95	0.05
Rostral anterior cingulate	0.02	0.32	0.16	0.03*	-1.36	0.18
Insula	-0.01	0.10	0.00	0.51	-1.33	0.19

Table 3. Statistics of ROI-based SA asymmetry for the human and chimpanzee brain. * denotes ROI's with significant asymmetry (i.e. $p < 0.05$ uncorrected for multiple comparisons), and ** denotes ROI's with highly significant asymmetry that survived the Bonferroni correction (i.e. $p < 0.05/34$).

Cortical Thickness ROIs	Human		Chimpanzee		Species Difference	
	AI	p-value	AI	p-value	t-stats	p-value
Frontal						
Superior frontal	0.02	0.00**	-0.00	-0.94	4.75	0.00**
Rostral middle frontal	0.03	0.00**	0.02	0.01*	0.95	0.34
Caudal middle frontal	0.00	0.34	-0.01	-0.45	1.20	0.23
Pars-opercularis	0.00	0.38	0.00	0.87	0.38	0.70
Pars-triangularis	-0.00	-0.61	0.01	0.31	-1.16	0.25
Pars-orbitalis	-0.02	-0.08	-0.01	-0.31	-0.29	0.78
Lateral orbito frontal	0.01	0.16	-0.01	-0.11	2.15	0.03*
Medial orbito frontal	0.00	0.93	-0.01	-0.41	0.72	0.47
Precentral	0.00	0.61	-0.03	-0.00**	3.84	0.00**
Paracentral	-0.02	-0.005*	-0.04	-0.00**	2.21	0.03*
Frontal pole	0.02	0.07	0.00	0.99	1.10	0.27
Parietal						
Superior parietal	0.01	0.14	-0.00	-0.42	1.58	0.12
Inferior parietal	-0.01	-0.02*	-0.00	-0.65	-0.94	0.35
Supramarginal	0.00	0.69	0.01	0.03*	-1.33	0.18
Postcentral	0.01	0.05	-0.00	-0.28	2.19	0.03*
Precuneus	-0.00	-0.98	0.03	0.00**	-3.67	0.00**
Temporal						
Middle temporal	-0.02	-0.00**	0.01	0.06	-3.88	0.00**
Inferior temporal	-0.02	-0.00**	-0.00	-0.81	-2.02	0.04*
Superior temporal	-0.02	-0.002*	-0.00	-0.64	-1.67	0.10
Bankssts	-0.03	-0.00*	0.00	0.83	-2.09	0.04*
Fusiform	-0.01	-0.03*	-0.01	-0.26	-0.26	0.79
Transverse temporal	-0.01	-0.55	-0.03	-0.01*	1.83	0.07
Entorhinal	-0.02	-0.06	-0.00	-0.83	-0.86	0.39
Temporal pole	-0.00	-0.75	-0.01	-0.71	0.16	0.88
Parahippocampal	-0.02	-0.01*	-0.04	-0.00**	1.28	0.20
Occipital						
Lateral occipital	-0.03	-0.00**	-0.02	-0.00**	-1.27	0.21
Lingual	-0.04	-0.00**	-0.01	-0.16	-3.26	0.00**
Cuneus	-0.03	-0.00**	0.00	0.97	-3.63	0.00**
Pericalcarine	-0.04	-0.00**	0.01	0.38	-3.70	0.00**
Cingulate & insula						
Caudal anterior cingulate	0.01	0.38	0.06	0.00**	-2.54	0.01*
Isthmus cingulate	-0.00	-0.97	-0.02	-0.08	1.33	0.18
Posterior cingulate	0.01	0.11	0.00	0.62	0.68	0.50
Rostral anterior cingulate	0.06	0.00**	0.05	0.01*	0.53	0.60
Insula	0.00	0.49	0.02	0.00**	-2.52	0.01*

Table 4. Statistics of ROI-based CT asymmetry index for the human and chimpanzee brain. * denotes ROI's with significant asymmetry (i.e. $p < 0.05$ uncorrected for multiple comparisons), and ** denotes ROI's with highly significant asymmetry that survived the Bonferroni correction (i.e. $p < 0.05/34$).

Figure Captions

Figure 1. Flow diagrams of the steps in the application of the single atlas parcellation scheme (SAPS), and two atlas parcellation scheme (TAPS), for vertex-wise (a and c) and ROI-based analyses (b and d) are shown in the left and right columns, respectively, for the case of an individual in the chimpanzee cohort. For the vertex-wise analysis in SAPS (a) the inter-hemispheric and between subject correspondences are established by co-registering both cerebral hemispheres of individual subjects to a symmetric registration atlas. For the corresponding vertex-wise analysis in TAPS (b) only between subject correspondences are established by separately co-registering left and right cerebral hemispheres of individual subjects to the relevant side of the atlas. For ROI-based analysis in SAPS (c) the parcellation of one cerebral hemisphere of the Desikan-Killiany atlas (e.g. left side) is first projected to both the ipsilateral and contralateral cerebral hemisphere of individual subjects. The pipeline is then repeated using the opposite side of the Desikan-Killiany atlas and the two results are averaged. For ROI-based analysis in TAPS (d) the parcellation convention of each cerebral hemisphere in the Desikan-Killiany atlas is propagated separately to the corresponding hemisphere of individual subjects. The illustration is simplified by showing only one half of the SAPS analysis pipeline for step-by-step comparison with TAPS.

Figure 2. Vertex-wise results of (a) SA and (b) CT asymmetry illustrating (i) significant asymmetries for the human (left) and chimpanzee brain (right), in which hot colours refer to leftward asymmetry and cool colours to rightward asymmetry and (ii) significant difference of asymmetry between the human and chimpanzee brain (middle), in which the intensity of the hot colour indicates the significance level of the difference. The highlighted areas survive the cluster-wise correction for multiple comparisons and the significance level of the respective cluster forming, and cluster-wise alphas are set as $p < 0.01$.

Figure 3. ROI-based results of (a) SA and (b) CT asymmetry illustrating (i) significant signed asymmetries across 34 ROIs for the human (left panel) and (ii) chimpanzee brain (right panel), in which hot colours refer to leftward asymmetry and cool colours to rightward asymmetry, and (iii) difference between species (middle panel), in which the intensity of the hot colour

1
2
3 indicates the significance level of the difference. Bonferroni correction is performed in ROI-
4 based analysis and the significance level is set as $p < 0.05/34$.
5
6
7
8
9

10 Figure 4. Vertex-wise average asymmetry maps of (a) SA and (b) CT. In each panel, the left
11 shows the result for the human brain and right for the chimpanzee brain. Hot colours
12 correspond to leftward asymmetry and cool colours to rightward asymmetry. The yellow
13 contours are drawn to identify regions of significant species difference.
14
15
16
17
18
19
20
21
22
23
24
25
26
27
28
29
30
31
32
33
34
35
36
37
38
39
40
41
42
43
44
45
46
47
48
49
50
51
52
53
54
55
56
57
58
59
60

For Peer Review

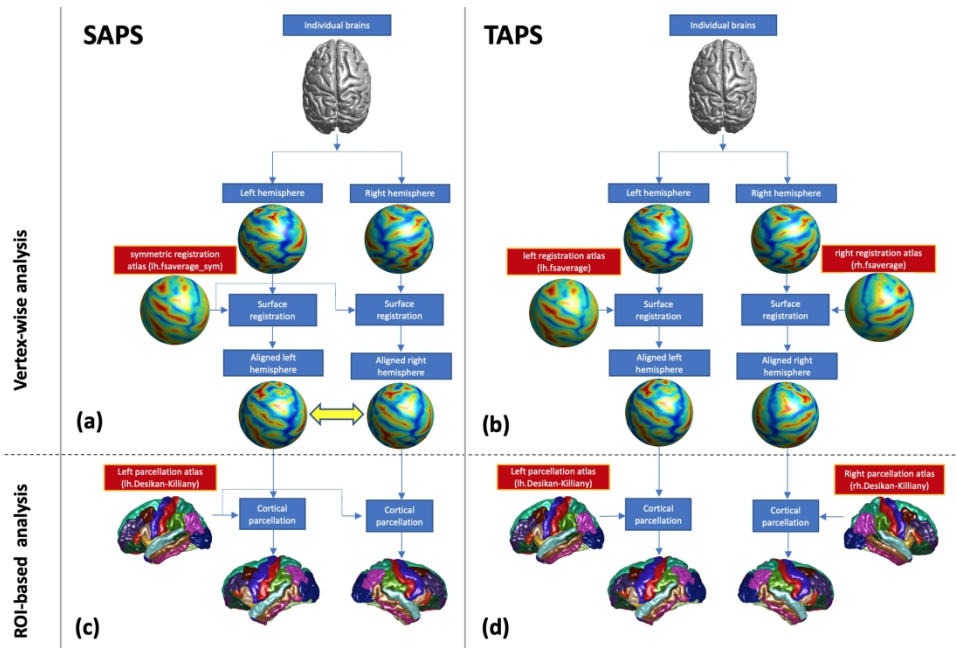


Figure 1. Flow diagrams of the steps in the application of the single atlas parcellation scheme (SAPS), and two atlas parcellation scheme (TAPS), for vertex-wise (a and c) and ROI-based analyses (b and d) are shown in the left and right columns, respectively, for the case of an individual in the chimpanzee cohort. For the vertex-wise analysis in SAPS (a) the inter-hemispheric and between subject correspondences are established by co-registering both cerebral hemispheres of individual subjects to a symmetric registration atlas. For the corresponding vertex-wise analysis in TAPS (b) only between subject correspondences are established by separately co-registering left and right cerebral hemispheres of individual subjects to the relevant side of the atlas. For ROI-based analysis in SAPS (c) the parcellation of one cerebral hemisphere of the Desikan-Killiany atlas (e.g. left side) is first projected to both the ipsilateral and contralateral cerebral hemisphere of individual subjects. The pipeline is then repeated using the opposite side of the Desikan-Killiany atlas and the two results are averaged. For ROI-based analysis in TAPS (d) the parcellation convention of each cerebral hemisphere in the Desikan-Killiany atlas is propagated separately to the corresponding hemisphere of individual subjects. The illustration is simplified by showing only one half of the SAPS analysis pipeline for step-by-step comparison with TAPS.

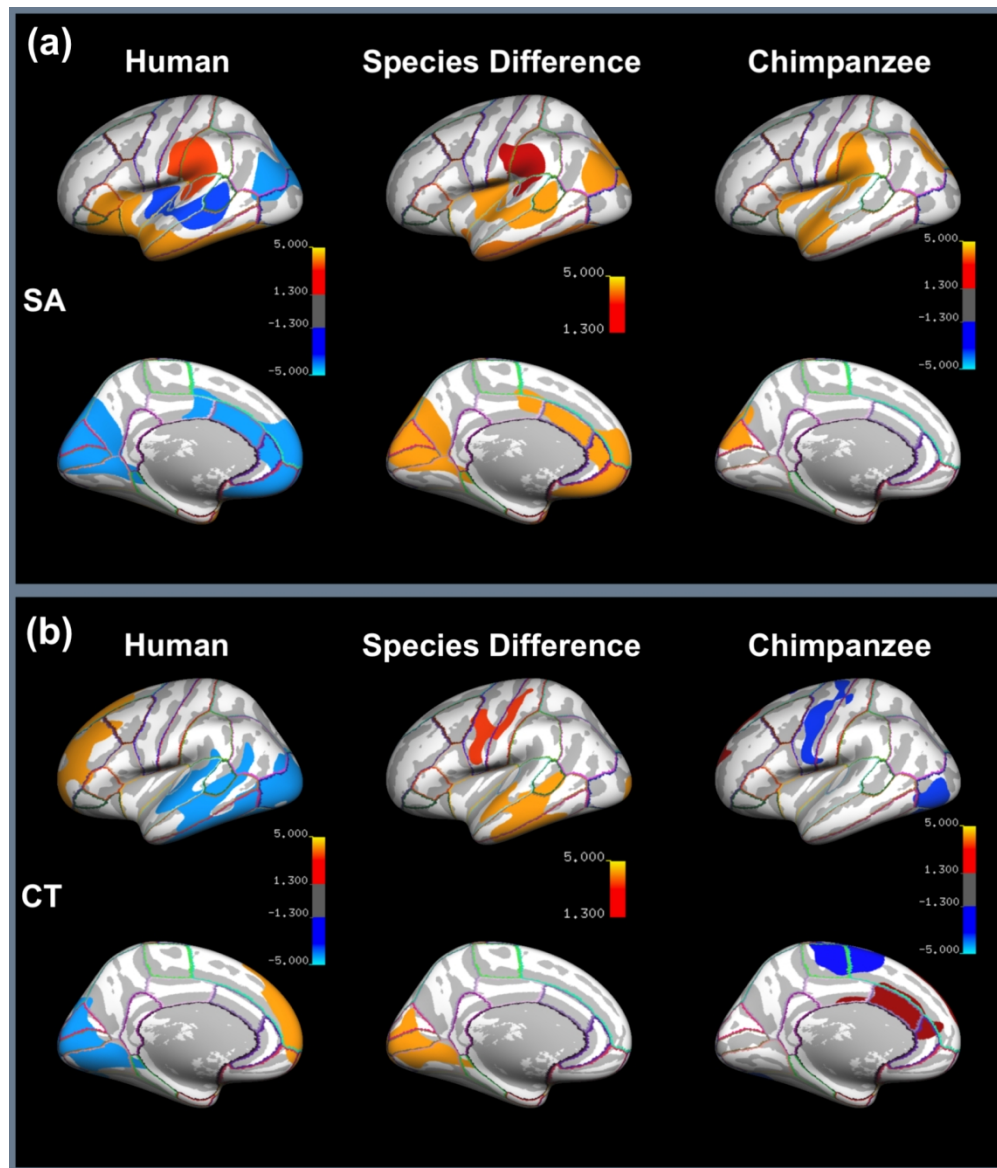


Figure 2. Vertex-wise results of (a) SA and (b) CT asymmetry illustrating (i) significant asymmetries for the human (left) and chimpanzee brain (right), in which hot colours refer to leftward asymmetry and cool colours to rightward asymmetry and (ii) significant difference of asymmetry between the human and chimpanzee brain (middle), in which the intensity of the hot colour indicates the significance level of the difference. The highlighted areas survived the cluster-wise correction for multiple comparisons and the significance level of the respective cluster forming, and cluster-wise alphas are set as $p < 0.01$.

643x750mm (72 x 72 DPI)

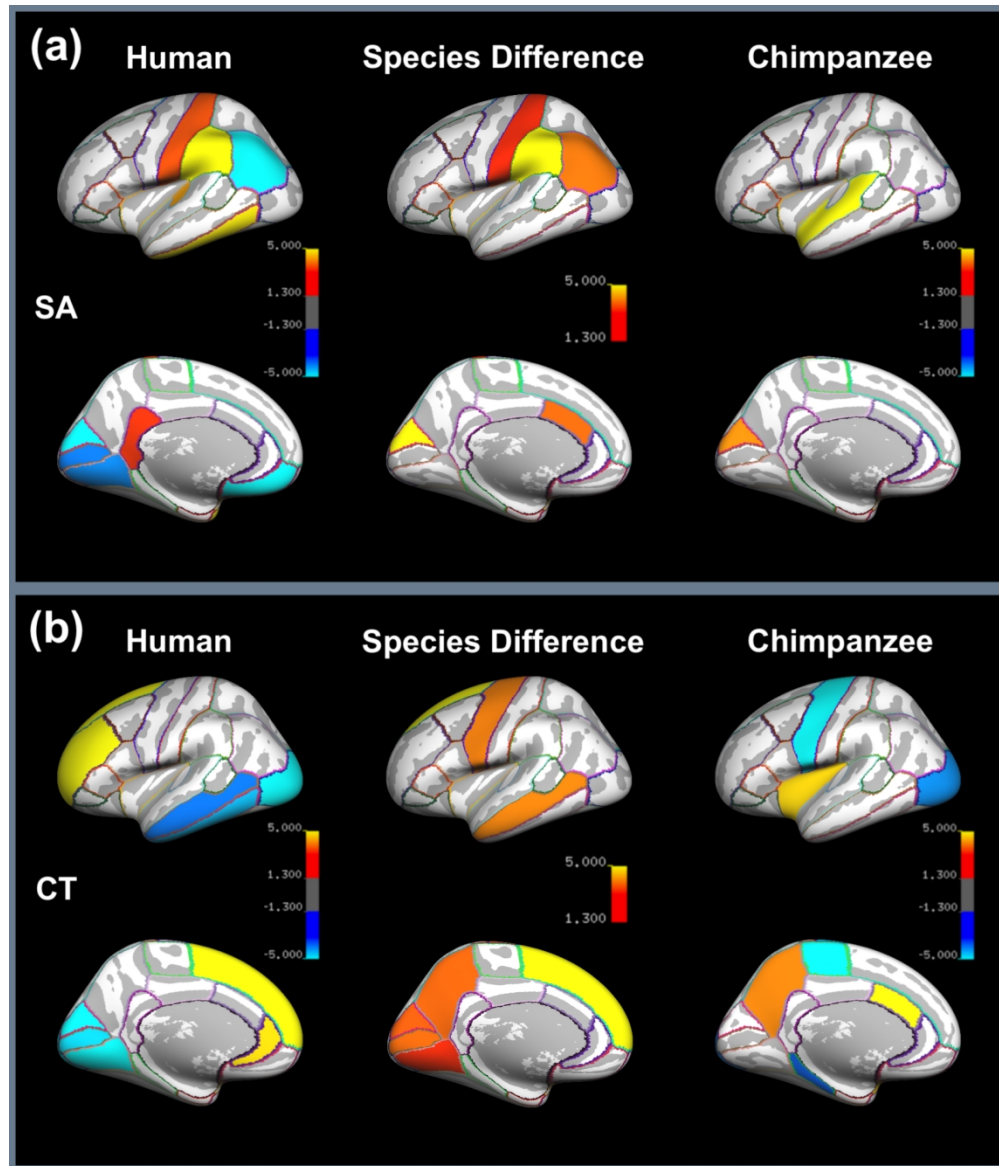


Figure 3. ROI-based results of (a) SA and (b) CT asymmetry illustrating (i) significant asymmetries across 34 ROIs for the human (left panel) and (ii) chimpanzee brain (right panel), in which hot colours refer to leftward asymmetry and cool colours to rightward asymmetry, and (iii) difference between species (middle panel), in which the intensity of the hot colour indicates the significance level of the difference. Bonferroni correction is performed in ROI-based analysis and the significance level is set as $p < 0.05/34$.

643x750mm (72 x 72 DPI)

1
2
3
4
5
6
7
8
9
10
11
12
13
14
15
16
17
18
19
20
21
22
23
24
25
26
27
28
29
30
31
32
33
34
35
36
37
38
39
40
41
42
43
44
45
46
47
48
49
50
51
52
53
54
55
56
57
58
59
60

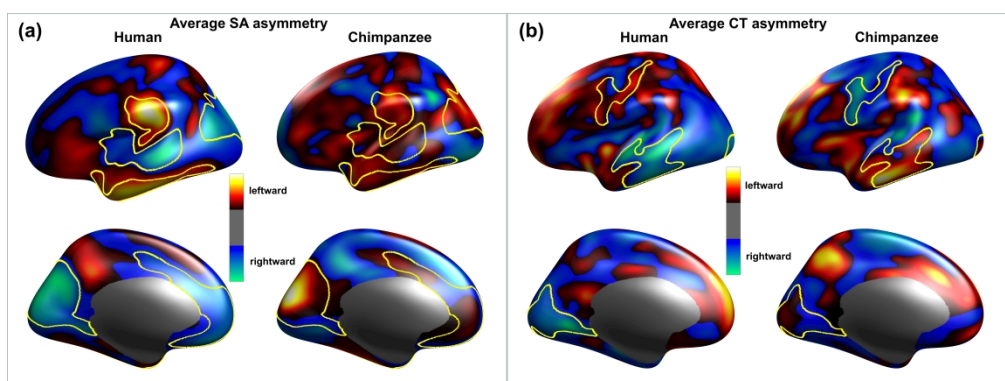


Figure 4. Vertex-wise average asymmetry maps of (a) SA and (b) CT. In each panel, the left shows the result for the human brain and right for the chimpanzee brain. Hot colours correspond to leftward asymmetry and cool colours to rightward asymmetry. The yellow contours are drawn to identify regions of significant species difference.

SUPPLEMENTARY MATERIALS

1 Evaluation of the effect of atlas-bias on ROI-based analysis of SA asymmetry

The FreeSurfer parcellation atlas, i.e. Desikan-Killiany atlas (Desikan et al., 2006) is asymmetric between the left and right cerebral hemisphere (see Figure S1 (a)). Being constructed by averaging the manual delineations of 34 ROIs that are defined by relevant gyri for each cerebral hemisphere on co-registered 3D MRI scans obtained for 40 individuals, the neuro-anatomical atlas carries the inherent asymmetry of the human brain. According to Figure S1 (b), significantly different numbers of vertices are assigned to corresponding ROIs of the left and right cerebral hemispheres of the Desikan-Killiany atlas, i.e., the inter-hemispheric difference is greater than 10% in ten regions, namely, caudal anterior cingulate, inferior parietal, transverse temporal, entorhinal, middle temporal, paracentral, pars-opercularis, pars-triangularis, rostral anterior cingulate and frontal pole. We hypothesised that the asymmetry in the atlas can cause systematic bias in the computation of brain asymmetry for individual subjects through differential distribution of vertices during the parcellation process if the conventional two-atlas based parcellation scheme (TAPS) is applied. An experiment was conducted to apply the Desikan-Killiany atlas to compute brain asymmetry using TAPS and SAPS, respectively. Specially, we randomly selected 3D MR images for 14 subjects from the human cohort and prepared a corresponding series of images for the same subjects which however, had been left-right flipped with respect to plane $x=0$ in the MNI space. The results of the average brain asymmetry for the original brain scans and their mirror reflections using the two schemes are shown in Figure S2.

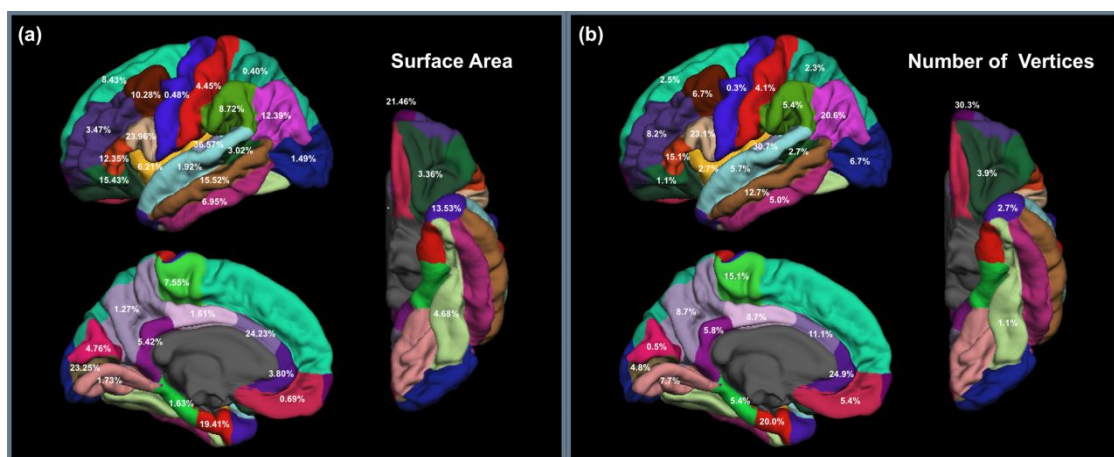


Figure S1. Atlas-bias computed as the normalized difference of (a) surface area and (b) number of vertices between corresponding ROIs of the left and right cerebral hemisphere.

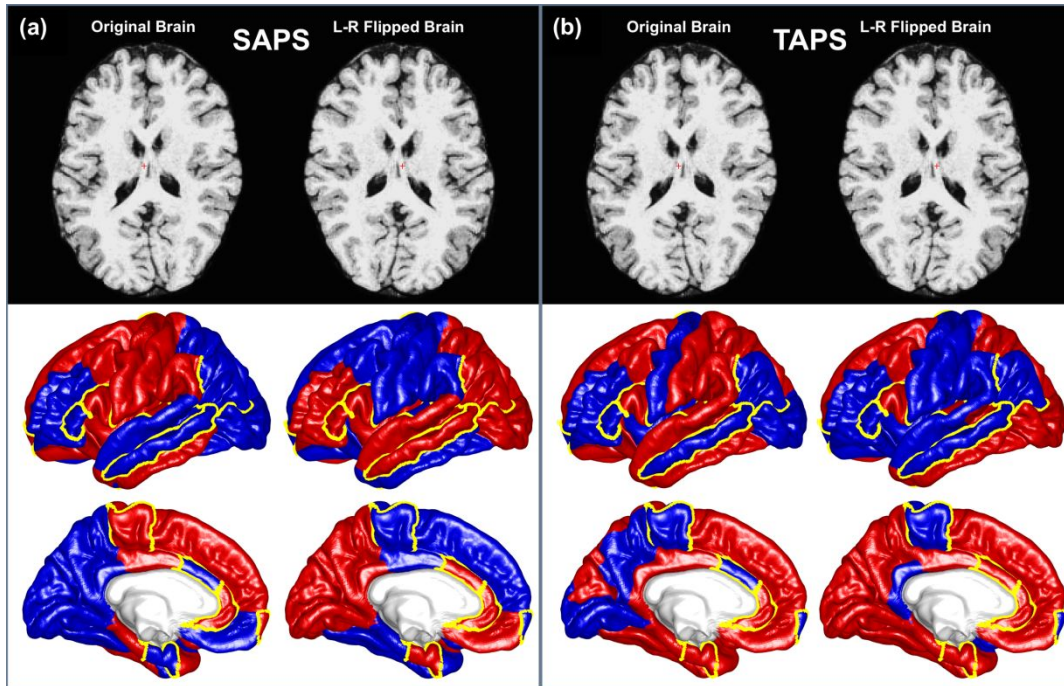


Figure S2. Results of SA asymmetry computed based on (a) SAPS in the present study and (b) TAPS in FreeSurfer illustrating the former provides more accurate and reliable results than the latter. In each panel, the top row demonstrates the orientation of the brain scan and the bottom shows the corresponding SA asymmetry; the left refers to average SA asymmetry of the brain images of 14 human subjects and the right refers to average SA asymmetry for the same 14 brain images analysed with the same respective atlas after being flipped left-right with respect to plane $x=0$ in the MNI space. Red colour denotes leftward asymmetry and blue colour rightward asymmetry. The regions with large inter-hemispheric parcellation difference (i.e. greater than 10%) are highlighted using yellow contour (see also Figure S1 (b)).

2 Regional parcellation for the chimpanzee brain

Examples for 10 randomly selected chimpanzee subjects are shown in Figure S3, which demonstrate that the Desikan-Killiany atlas provides reasonable parcellation results for the chimpanzee brain.

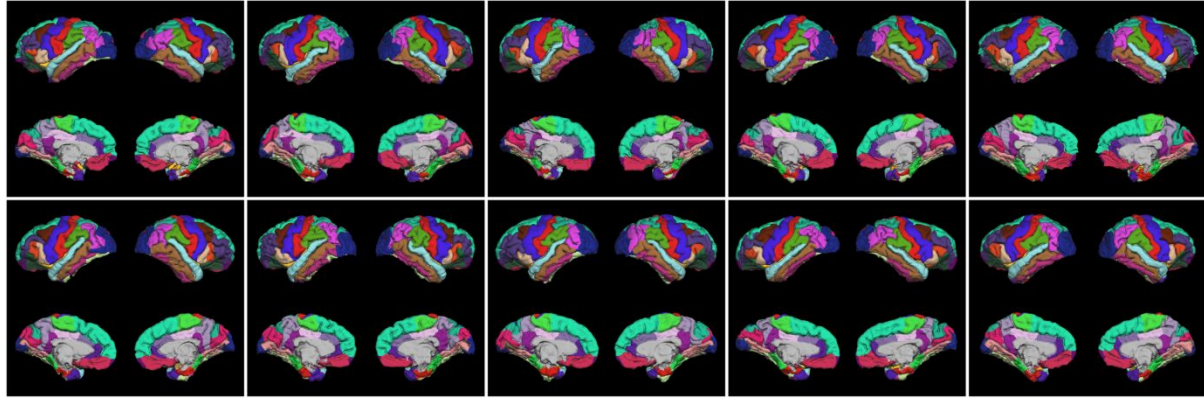


Figure S3. The automatic cortical parcellation for 10 brains randomly selected from the chimpanzee cohort demonstrating excellent correspondence between the boundaries of the ROIs propagated from the human Desikan-Killiany atlas.

3 ROI-based cortical measurements for the human and chimpanzee brains

Surface Area ROIs	Human				Chimpanzee			
	Left Hemisphere		Right Hemisphere		Left Hemisphere		Right Hemisphere	
	mean	SD	mean	SD	mean	SD	mean	SD
Frontal								
Superior frontal	9160.20	1215.23	9312.63	1187.96	2822.15	242.25	2806.18	241.21
Rostral middle frontal	7683.78	1095.67	7844.30	1168.82	1772.58	244.74	1792.42	267.16
Caudal middle frontal	2743.60	506.44	2717.71	481.18	854.05	102.75	848.92	103.13
Pars-opercularis	2188.76	373.04	2169.89	392.17	693.75	99.51	693.84	109.61
Pars-triangularis	1896.33	289.30	1856.14	314.18	497.73	109.06	500.65	112.94
Pars-orbitalis	1181.31	126.01	1172.71	156.98	234.46	34.74	239.04	41.22
Lateral orbito frontal	3421.74	464.57	3383.83	454.92	1042.83	284.75	1007.88	285.93
Medial orbito frontal	2778.06	400.27	3089.12	767.53	1482.83	571.62	1480.29	622.98
Precentral	5659.86	683.81	5745.99	707.24	2415.99	196.69	2438.51	208.01
Paracentral	1635.95	235.37	1615.58	243.57	675.51	51.26	687.56	64.33
Frontal pole	472.20	72.05	482.30	76.55	160.92	17.71	160.80	19.86
Parietal								
Superior parietal	6626.01	840.76	6821.43	843.29	2183.66	203.79	2165.68	193.46
Inferior parietal	6193.94	859.28	6515.50	826.72	1887.03	182.54	1890.72	178.93
Supramarginal	4876.03	838.11	4436.49	882.30	1480.99	119.07	1466.08	121.88
Postcentral	5361.64	671.55	5181.26	608.15	2125.51	159.00	2130.29	173.24
Precuneus	4723.62	586.59	4790.12	619.13	1396.37	170.15	1409.70	182.28
Temporal								
Middle temporal	5036.97	683.12	5064.09	695.45	1459.38	172.32	1444.59	162.84
Inferior temporal	4974.64	710.57	4764.04	661.39	1277.37	152.59	1261.80	165.81
Superior temporal	4927.07	695.35	4827.50	599.52	1739.34	141.96	1679.95	126.64
Bankssts	1060.86	203.68	1110.63	202.06	180.74	19.72	183.66	23.04
Fusiform	4425.63	487.97	4425.54	476.65	1138.12	138.86	1128.37	180.16
Transverse temporal	546.02	119.69	503.17	90.96	148.72	19.02	145.65	17.73
Entorhinal	881.97	194.09	903.52	189.91	402.76	192.52	441.88	267.44
Temporal pole	873.88	111.82	815.78	101.82	333.26	54.69	325.25	45.87
Parahippocampal	1184.63	183.05	1185.68	205.07	588.51	251.39	614.45	347.94
Occipital								
Lateral occipital	5825.57	778.85	5920.21	864.59	2116.63	193.97	2172.38	260.93
Lingual	3754.40	476.37	3869.47	466.32	1302.34	254.80	1302.08	234.07
Cuneus	1813.12	220.92	1977.91	263.27	752.98	121.57	695.94	137.91
Pericalcarine	1472.42	288.75	1562.72	322.91	694.01	146.55	695.10	157.60
Cingulate & Insula								
Caudal anterior cingulate	979.53	220.59	1113.93	555.48	182.51	32.10	172.87	27.20
Isthmus cingulate	1477.15	508.80	1367.37	334.86	592.32	153.24	586.92	116.43
Posterior cingulate	1381.77	202.99	1439.18	276.60	481.14	52.23	479.08	57.70
Rostral anterior cingulate	1230.78	218.05	1261.12	583.52	491.07	157.80	462.00	214.64
Insula	2589.88	383.01	2636.68	447.67	1014.15	181.94	997.35	174.74

Table S1. Statistics of mean and standard deviation of regional surface area measurement for the human and chimpanzee brains.

Cortical Thickness ROIs	Human				Chimpanzee			
	Left Hemisphere		Right Hemisphere		Left Hemisphere		Right Hemisphere	
	mean	SD	mean	SD	mean	SD	mean	SD
Frontal								
Superior frontal	2.61	0.14	2.55	0.14	1.96	0.16	1.96	0.17
Rostral middle frontal	2.26	0.14	2.20	0.15	1.62	0.12	1.59	0.13
Caudal middle frontal	2.39	0.15	2.38	0.15	1.63	0.20	1.64	0.18
Pars-opercularis	2.48	0.14	2.47	0.15	1.72	0.16	1.72	0.17
Pars-triangularis	2.37	0.15	2.38	0.16	1.71	0.15	1.70	0.19
Pars-orbitalis	2.65	0.21	2.69	0.23	1.98	0.20	2.01	0.19
Lateral orbito frontal	2.57	0.16	2.55	0.17	2.02	0.15	2.04	0.15
Medial orbito frontal	2.27	0.18	2.27	0.16	1.65	0.18	1.66	0.17
Precentral	2.32	0.17	2.31	0.16	1.37	0.20	1.41	0.19
Paracentral	2.11	0.15	2.15	0.15	1.35	0.18	1.40	0.17
Frontal pole	2.79	0.29	2.73	0.28	1.77	0.25	1.77	0.22
Parietal								
Superior parietal	2.09	0.11	2.08	0.12	1.30	0.10	1.30	0.08
Inferior parietal	2.34	0.12	2.36	0.12	1.38	0.13	1.38	0.12

Supramarginal	2.49	0.13	2.48	0.14	1.58	0.14	1.56	0.14
Postcentral	1.98	0.10	1.96	0.12	1.23	0.09	1.23	0.09
Precuneus	2.27	0.14	2.27	0.12	1.35	0.13	1.31	0.12
Temporal								
Middle temporal	2.75	0.17	2.81	0.16	1.64	0.14	1.62	0.13
Inferior temporal	2.69	0.16	2.74	0.17	1.58	0.13	1.59	0.13
Superior temporal	2.68	0.15	2.72	0.15	1.45	0.15	1.46	0.14
Bankssts	2.44	0.16	2.51	0.19	1.37	0.19	1.36	0.18
Fusiform	2.56	0.18	2.58	0.16	1.33	0.10	1.34	0.11
Transverse temporal	2.32	0.20	2.33	0.19	1.24	0.19	1.28	0.17
Entorhinal	3.18	0.32	3.24	0.31	1.93	0.25	1.94	0.27
Temporal pole	3.61	0.27	3.63	0.30	2.15	0.26	2.16	0.26
Parahippocampal	2.45	0.22	2.50	0.20	1.23	0.16	1.28	0.17
Occipital								
Lateral occipital	2.13	0.12	2.18	0.13	1.19	0.09	1.21	0.07
Lingual	1.86	0.13	1.94	0.14	1.10	0.09	1.11	0.09
Cuneus	1.75	0.13	1.81	0.13	1.18	0.09	1.18	0.09
Pericalcarine	1.54	0.15	1.59	0.16	1.06	0.11	1.05	0.11
Cingulate & Insula								
Caudal anterior cingulate	2.27	0.27	2.24	0.23	1.39	0.20	1.31	0.18
Isthmus cingulate	2.16	0.19	2.16	0.17	1.44	0.15	1.47	0.13
Posterior cingulate	2.33	0.16	2.30	0.15	1.41	0.14	1.41	0.16
Rostral anterior cingulate	2.69	0.24	2.54	0.26	1.07	0.27	1.02	0.26
Insula	2.94	0.16	2.93	0.17	1.90	0.12	1.86	0.14

Table S2. Statistics of mean and standard deviation of regional cortical thickness measurement for the human and chimpanzee brains.

4 CT asymmetry computed based on FWHM filter sizes of 15, 10 and 5 mm

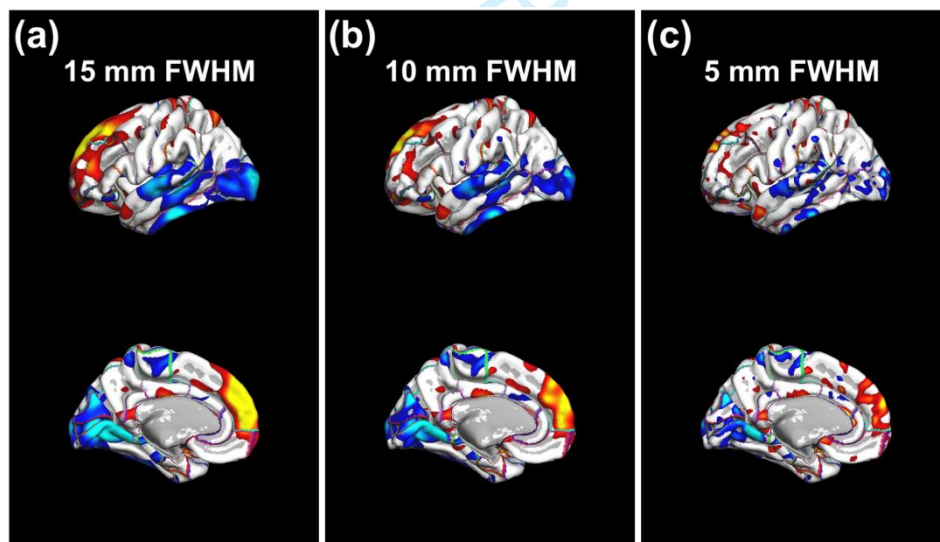


Figure S4. Significant CT asymmetry maps ($p < 0.05$) computed with FWHM spatial filter size of (a) 15 mm, (b) 10 mm and (c) 5 mm showing (i) consistency in the asymmetry pattern for the human brain and (ii) 15 mm corresponds well with the size of brain petalia and gyri which are the features that are the focus of interest in the study. Hot colours refer to leftward asymmetry and cool colours to rightward asymmetry.